MODELING SENSORINEURAL HEARING LOSS

Edited by

Walt Jesteadt

Modeling Sensorineural Hearing Loss

Modeling Sensorineural Hearing Loss

Edited by
Walt Jesteadt
Boys Town National Research Hospital

Routledge
Taylor & Francis Group
LONDON AND NEW YORK

First published 1997 by Lawrence Erlbaum Associates, Inc.

Published 2018 by Routledge
2 Park Square, Milton Park, Abingdon, Oxon OX14 4RN
52 Vanderbilt Avenue, New York, NY 10017

First issued in paperback 2018

Routledge is an imprint of the Taylor & Francis Group, an informa business

Library of Congress Cataloging-in-Publication-Data

Modeling sensorineural hearing loss / edited by Walt Jesteadt
p. cm.
Includes bibliographic references and index.
ISBN 0-8058-2230-5 (alk. paper)
1. Deafness—Mathematical models. 2. Auditory perception—Mathematical models. 3. Deafness—Computer simulation. I. Jesteadt, Walt.
RF291.M55 1997
617.8'001'1—dc21 96-49676
CIP

ISBN 13: 978-1-138-87660-6 (pbk)
ISBN 13: 978-0-8058-2230-4 (hbk)

CONTENTS

Preface xi

Introduction: Modeling Sensorineural Hearing Loss
Walt Jesteadt 1

SECTION I:
PHYSIOLOGICAL AND PERCEPTUAL MODELS OF SENSORINEURAL HEARING LOSS

Introduction
Stephen T. Neely 6

1 Cochlear Excitation Patterns in Sensorineural Hearing Loss
Eric Javel 9

2 Representation of the Vowel /eh/ in the Auditory Nerve of Cats With a Noise-Induced Hearing Loss
Roger L. Miller, John R. Schilling, Eric D. Young, and Kevin R. Franck 35

3 A Computational Model of Reorganization in Auditory Cortex in Response to Cochlear Lesions
Rick L. Jenison 49

4 Implementation of the MBPNL Nonlinear Cochlear I/O Model in the C Programming Language, and Applications for Modeling Impaired Auditory Function
Tai Lin and Julius L. Goldstein 67

5 Using a Cochlear Model to Develop Adaptive Hearing-Aid Processing
James M. Kates 79

SECTION II:
SIMULATION AND COMPENSATION
FOR REDUCED DYNAMIC RANGE

Introduction
Larry E. Humes 94

6 Derecruitment by Multiband Compression in Hearing Aids
Jont B. Allen 99

7 DSP Implementation of a Real-Time Hearing Loss Simulator Based on Dynamic Expansion
David S. Lum and Louis D. Braida 113

8 Effects of Linear Amplification and Amplitude Compression on Sentence Reception by Listeners With Hearing Loss Simulated by Masking Noise
Steven V. De Gennaro and Louis D. Braida 131

9 Voiced Stop Consonant Discrimination With Multichannel Expansion Hearing Loss Simulations
E. William Yund and Thomas R. Crain 149

SECTION III:
LOUDNESS GROWTH AND INTENSITY
DISCRIMINATION AS MEASURES
OF NONLINEARITY

Introduction
Louis D. Braida 170

10 Modeling Loudness Growth and Loudness Summation in Hearing-Impaired Listeners
Stefan Launer, Volker Hohmann, and Birger Kollmeier 175

11 A Model of Loudness Summation Applied to High-Frequency Hearing Loss
Mary Florentine, Søren Buus, and Rhona P. Hellman 187

12 Growth of Loudness in Sensorineural Impairment: Experimental Results and Modeling Implications
Rhona P. Hellman 199

13 Relation Between the Rate of Growth of Loudness and the Intensity DL
Stephen T. Neely and Jont B. Allen 213

14 On the Role and Structure of the Decision Variable Variance Function in Modeling Intensity Discrimination in Normal Hearing and Simulated Hearing Loss
William S. Hellman 223

15 Modeling Level Discrimination of Broadband Signals by Listeners With Sensorineural Hearing Loss
Robert A. Lutfi and Karen A. Doherty 235

SECTION IV:
ADDITIVITY OF MASKING AS A MEASURE OF NONLINEARITY

Introduction
Marjorie R. Leek 248

16 Additivity of Multiple Maskers of Speech
Judy R. Dubno and Jayne B. Ahlstrom 253

17 Modeling the Effects of Peripheral Nonlinearity in Listeners With Normal and Impaired Hearing
Andrew J. Oxenham and Brian C. J. Moore 273

18 Modeling Hearing Loss as an Additional Source of Masking
Walt Jesteadt, Donna L. Neff, Larry E. Humes, and Marjorie R. Leek 289

SECTION V: SPECTRAL AND TEMPORAL PROCESSING IN SENSORINEURAL HEARING LOSS

Introduction
Søren Buus 308

19 Simulation of Sensorineural Hearing Loss: Reducing Frequency Resolution by Uniform Spectral Smearing
Arthur Boothroyd, Bethany Mulhearn, Juan Gong, and Jodi Ostroff 313

20 Evaluation of a Scheme to Compensate for Reduced Frequency Selectivity in Hearing-Impaired Subjects
Thomas Baer and Brian C. J. Moore 329

21 Timbre Discrimination by Hearing-Impaired Listeners
Marjorie R. Leek and Van Summers 343

22 Measurement and Modeling of Modulation Detection for Normal and Hearing-Impaired Listeners
C. Formby and T. G. Forrest 359

23 Measurement and Modeling of Temporal Gap Detection for Normal and Meniere Listeners
T. G. Forrest, C. Formby, and L. P. Sherlock 373

24 Temporal Masking and the "Active Process" in Normal and Hearing-Impaired Listeners
Christopher W. Turner and Karen A. Doherty 387

25 Application of Interaural Difference Models to Binaural Performance by Listeners with Hearing Impairments
Monica L. Hawley and H. Steven Colburn 397

SECTION VI: SPEECH PERCEPTION IN LISTENERS WITH SENSORINEURAL HEARING LOSS

Introduction
Judy R. Dubno 416

26 Prediction of Speech Reception by Listeners With Sensorineural Hearing Loss
Christine M. Rankovic 421

27 Prediction of Speech Recognition From Audibility and Psychoacoustic Abilities of Hearing-Impaired Listeners
Teresa Ching, Harvey Dillon, and Denis Byrne 433

28 Speech Intelligibility Prediction in Hearing-Impaired Listeners for Steady and Fluctuating Noise
Inga Holube, Matthias Wesselkamp, Wouter A. Dreschler, and Birger Kollmeier 447

29 Speech Perception in Noise by Listeners With Hearing Impairment and Simulated Sensorineural Hearing Loss
Alyssa R. Needleman and Carl C. Crandell 461

30 Influence of Relative Amplitude and Presentation Level on Perception of the /p/ – /t/ Stop Consonant Contrast by Normal and Impaired Listeners
Mark S. Hedrick and Walt Jesteadt 475

Author Index 487

Subject Index 495

PREFACE

This book began with efforts by Larry Humes and myself to summarize published data concerning masking and loudness perception in listeners with sensorineural hearing loss, for use in model development or meta-analyses. There were, of course, many more sets of data than we could process, along with a broad array of related models, so we began looking for other ways to gather and coalesce this information.

At the 1994 meeting of the Association for Research in Otolaryngology, I talked to people with similar interests about holding an open conference to discuss issues related to modeling sensorineural hearing loss. This group developed into an organizing committee consisting of Jont Allen, Louis Braida, Søren Buus, Judy Dubno, Mary Florentine, Larry Humes, Eric Javel, Marjorie Leek, Donna Neff, Stephen Neely, and Christopher Turner. They provided input on a wide range of issues and formed a core group of active participants. A conference on modeling sensorineural hearing loss was held at Boys Town, Nebraska, on June 10–11, 1995. Preprints were circulated in advance, and then revised to incorporate discussions at the conference and appropriate references to related work presented there. The revised versions appear as chapters in this book.

We have maintained the division into six sections that was used for the conference itself. Because this was an open conference rather than one with invited speakers, many chapters are closely related. The variety of approaches taken by different authors and the narrow focus of the subject matter made the organization of chapters into sections somewhat arbitrary. Members of the organizing committee who chaired sessions have written introductions to the corresponding sections of the book that highlight the central issues. This book provides an excellent overview of the current status of quantitative models of sensorineural hearing loss at the physiological and perceptual levels.

The conference was held under the auspices of the Continuing Education program of the Center for Hearing Loss in Children, a National Research and Training Center funded by the National Institute on Deafness and Other

Communication Disorders (P60 DC00982). My own contributions to the conference and to this book were supported in part by NIH (R01 DC00136). The very able and experienced Continuing Education staff, including Mary Pat Moeller, Gail Binderup, Barbara Grandfield, Skip Kennedy, and Diane Schmidt, handled all of the conference details. Barbara Olmedo, Coordinator of Research Administration at the Boys Town National Research Hospital, and Carole Dugan, an administrative assistant, handled preprint preparation, collection of final manuscripts, and conversion of computer files into a common machine-readable format. Neither the conference nor the book would have been possible without their help.

—Walt Jesteadt

INTRODUCTION
Modeling Sensorineural Hearing Loss

Walt Jesteadt
Boys Town National Research Hospital

A recent study indicated that 20 million people in the United States (8.4% of the population) have significant sensorineural hearing loss (Holt & Hotto, 1994). Approximately 95% of those people have partial losses, with varying degrees of residual hearing (Holt & Hotto, 1994). These percentages are similar in other developed countries. What changes in the function of the cochlea or inner ear cause such losses? What does the world sound like to the 19 million people with residual hearing? How should we transform sounds to correct for the hearing loss and maximize restoration of normal hearing?

Answers to such questions require detailed models of the way sounds are processed by the nervous system, both for listeners with normal hearing and for those with sensorineural hearing loss. A conference to discuss ongoing efforts to model sensorineural hearing loss was held at Boys Town, Nebraska, in June 1995. This book contains 30 chapters describing the work of 25 different research groups presented at the conference. The chapters have been grouped into six sections organized around different aspects of the problem. Each section begins with an introduction that highlights the central issues.

Section I includes a series of physiological studies of sensorineural hearing loss, beginning with a very general model for prediction of responses in the auditory nerve in the presence of hearing loss. It also includes two general models of perception in the presence of sensorineural hearing loss, focusing on nonspeech and speech signals. These chapters

were chosen for inclusion in the first section because they illustrate many of the basic principles or common elements in current models.

In general terms, most models assume a compressive nonlinearity in the mechanical response of the normal cochlea, which serves to map a large range of sound intensities into a much narrower range of neural responses. Sensorineural hearing loss is assumed to involve a reduction in the degree of peripheral nonlinearity as well as a threshold elevation, such that a narrower range of audible sounds is mapped into an approximately normal range of neural responses. Although changes in the mechanical response of the cochlea are a central factor in such models, there has been very little discussion of the effect of different forms of cochlear damage on cochlear mechanics per se. In meetings devoted to cochlear mechanics over the past 11 years, for example, only Allen (1990) and Ruggero and Rich (1990) addressed issues related to hearing loss. The standard assumptions concerning altered cochlear mechanics associated with hearing loss are based primarily on physiological data. Models of perception in the presence of hearing loss are generally based on physiological data as well.

The most obvious change associated with sensorineural hearing loss, readily observable at both the physiological and perceptual levels, is the reduced dynamic range of the system in frequency regions with significant threshold elevations. Section II of the book describes a series of related efforts to model this reduced dynamic range. Strategies include the use of masking noise and the introduction of an expansive nonlinearity to simulate the effects of hearing loss in listeners with normal hearing, for both speech and nonspeech stimuli.

Section III contains chapters concerned with the effects of dynamic range on loudness growth and intensity discrimination. These are two of the most common measures of altered dynamic range, and both measures have been used clinically to distinguish between conductive losses (characterized by threshold shifts without a change in dynamic range) and more complicated sensorineural losses. The presence of several chapters with similar titles illustrates the high level of interest and activity in this area in recent years, concentrated primarily on the relation between loudness and intensity discrimination.

There are many examples in the book in which masking noise is used as a means of creating a threshold elevation in normal listeners that is equivalent to that observed in a specific listener with hearing loss. This frequently leads to comparisons between results obtained with one masker or two for listeners with normal hearing, or comparisons between results obtained with only one masker for a listener with sensorineural hearing loss and those obtained with two maskers for listeners with normal hearing. Unfortunately, combination rules for multiple maskers are not at all clear, even for listeners with normal hearing, and these rules

may be different in the presence of hearing loss. Chapters in Section IV discuss results obtained with multiple maskers and what these results might tell us about peripheral nonlinearity.

Although many recent efforts to model sensorineural hearing loss have focused on alterations in the dynamic range or in the pattern of growth of neural response, there are many reports of altered frequency selectivity and impaired temporal processing as well. Chapters in Section V describe recent efforts to measure and model some of these effects. Of particular interest are cases in which reduced frequency selectivity leads to improved temporal processing.

Chapters throughout the book deal with various aspects of speech perception, beginning in Section I with the representation of speech in the responses of single auditory nerve fibers. Chapters in Section VI describe a number of closely related efforts to determine the extent to which speech perception deficits in listeners with sensorineural hearing loss can be accounted for on the basis of their elevated thresholds alone.

In many chapters, assumptions about altered peripheral processing are tested by modifying the input stimuli in accordance with a specific model. There are many ways of modeling hearing loss and of testing those models, but modification of the input stimuli represents the most direct approach to answering the questions in the first paragraph: What does the world sound like to those with hearing loss, and what could be done to restore normal perception? There are at least three ways to modify input stimuli, however, and it may help to compare them because the three categories represent an alternative scheme for grouping many of the chapters.

In the first category, the goal is to test models of altered peripheral processing by making an optimum correction to the input signal presented to listeners with normal hearing to *duplicate* the transformation imposed by the hearing loss. If assumptions about the nature of the hearing loss are valid, results obtained from listeners with normal hearing given corrected input will look more like those obtained from listeners with sensorineural hearing loss. Examples of this strategy include chapter 7 by Lum and Braida and chapter 9 by Yund and Crain in Section II, and chapter 19 by Boothroyd, Mulhearn, Gong, and Ostroff in Section V. In addition to testing a specific model, studies of this kind tell us what things might sound like to people with sensorineural hearing loss. Accurate simulations would be very helpful to those who interact with hearing-impaired people.

In the second category, the goal is to test models of altered peripheral processing by making an optimum correction to the input signal presented to listeners with sensorineural hearing loss to *compensate* for the nonlinear transformation imposed by the hearing loss. If assumptions concerning the nature of the hearing loss are valid, results obtained from listeners with sensorineural hearing loss given corrected input will look more like

those obtained from listeners with normal hearing. Examples of this strategy are presented in chapter 5 by Kates in Section I and chapter 20 by Baer and Moore in Section V. In addition to providing a test of a specific model, studies of this kind provide insights that may be useful in the design of hearing aids.

In the third category, masking noise is added to stimuli presented to listeners with normal hearing to simulate the elevated thresholds associated with sensorineural hearing loss, but the signal itself is not changed. This approach is closer to the first category listed previously than to the second. The goal in this case is to control for audibility of all portions of the signal waveform without making assumptions about changes in nonlinearity associated with hearing loss. To the extent that results obtained from listeners with normal hearing tested in noise look like those obtained from listeners with sensorineural hearing loss tested in quiet, changes in suprathreshold nonlinearity in the latter group may not be as important as the change in threshold itself. Interpretation of the results is not as straightforward as one might hope, however, because use of masking noise appears to alter the suprathreshold nonlinearity and can lead to other complications. These issues are discussed in chapter 16 by Dubno and Ahlstrom, chapter 17 by Oxenham and Moore, and chapter 18 by Jesteadt, Neff, Humes, and Leek in Section IV.

A great deal of research in recent years has been aimed at obtaining a better physiological description of the altered processes that cause sensorineural hearing loss, and a better understanding of transformations that occur in the perception of those sounds that are sufficiently intense that they can still be heard. Efforts to understand these changes in function have led to a better understanding of normal function as well. This research has been based on rigorous mathematical models, computer simulations of mechanical and physiological processes, and signal processing simulations of the altered perceptual experience of listeners with sensorineural hearing loss. This book provides examples of all of these approaches to modeling sensorineural hearing loss and a summary of the latest research in the field.

REFERENCES

Allen, J. A. (1990). Modeling the noise damaged cochlea. In P. Dallos, C. D. Geisler, J. W. Matthews, M. A. Ruggero, & C. R. Steele (Eds.), *The mechanics and biophysics of hearing* (pp. 324–332). Berlin: Springer-Verlag.

Holt, J. A., & Hotto, S. A. (1994). *Demographic aspects of hearing impairment: Questions and answers*. Washington, DC: Gallaudet University Center for Assessment and Demographic Studies.

Ruggero, M. A., & Rich, N. C. (1990). Systemic injection of furosemide alters the mechanical response to sound of the basilar membrane. In P. Dallos, C. D. Geisler, J. W. Matthews, M. A. Ruggero, & C. R. Steele (Eds.), *The mechanics and biophysics of hearing* (pp. 314–321). Berlin: Springer-Verlag.

I

PHYSIOLOGICAL AND PERCEPTUAL MODELS OF SENSORINEURAL HEARING LOSS

Introduction

Stephen T. Neely
Boys Town National Research Hospital

Hearing loss can be viewed as a deviation from the normal physiology of the auditory system. Models of the auditory system not only provide means for understanding normal physiology, they can also be manipulated to simulate the physiological impairments thought to be associated with hearing loss. The five chapters in Section I describe the simulation of hearing impairment using two types of auditory system models: animal and computational.

Animal models allow direct physiological measurements under controlled conditions. They can be manipulated directly or can be used to provide data for the construction of computational models. Observations of animal models allow us to make inferences about the human auditory system; however, caution is warranted due to inevitable differences between the animal model and the human ear. For example, the audible frequency range for a cat, the most frequently used animal model for auditory experiments, is somewhat higher (50 Hz to 50 kHz) than that for the human ear (20 Hz to 20 kHz). Another limitation is that the physiological state of the auditory systems may degrade during the measurement process.

Computational models are based primarily on data obtained from physiological measurements of animal models and, to a lesser extent, on psychophysical measurements. Computational models can aid our understanding of the auditory system by providing a framework in which information from many different sources is combined. Computational

models have the advantage of repeatability, due to their deterministic nature, and permit manipulation of any internal variable. However, these models are always imprecise, because of the incomplete knowledge of the auditory system; the difficulty of analyzing nonlinear, dynamic systems; and the need to control computational complexity.

In the first chapter in this section, Javel describes a computational model of the cat inner ear that simulates neuronal responses to arbitrary signals. This model is based primarily on data from the measurement of neuronal responses in cats to tone bursts at various frequencies and levels. Aspects of middle-ear and cochlear mechanics are also included. Various forms of sensorineural or conductive hearing loss can be simulated in this model by modifying appropriate components. As a demonstration, the model's normal response to the vowel /eh/ is shown to be similar to measurements in cats (Young & Barta, 1986). Model responses are also presented for a simulated hearing loss, with and without a simulated hearing aid.

In the second chapter, Miller, Shilling, Franck, and Young present the results of physiological measurements using the cat as an animal model. A hearing loss was induced by exposure to a narrow band of noise. Single nerve-fiber responses to the vowel /eh/ in the impaired ears were compared with normal responses. Normal animals show a capture phenomenon in which the formant frequencies increasingly dominate the responses as the level is increased (Young & Sachs, 1979). The impaired responses do not show capture by formants. The loss of capture is thought to reflect not only broadened tuning, but also a weakening of cochlear suppression. Two-tone suppression has been shown to be reduced in regions of outer-hair-cell loss (Schmiedt, Mills, & Adams, 1990).

In the third chapter, Jenison uses a computational model at the level of the auditory cortex to investigate plasticity of the sensory map in response to a cochlear lesion. A computational neural network is used to simulate neural connections between the cochlea and a two-dimensional surface representing the auditory cortex. The cochlear output was provided by a model of the peripheral auditory system developed in a previous study (Jenison, Greenberg, Kluender, & Rhode, 1991). The neural network was allowed to adapt first to normal cochlear output and then to the output of a cochlea with a notch hearing loss. Connection patterns in both cases were observed to be consistent with results from measurements of the responses of cortical neurons. An important finding of this study is that physical rewiring of the afferent projections is unnecessary to achieve the simulated reorganization of cortical connections, suggesting that reorganization occurs through local interactions that induce synaptic change.

In the fourth chapter, Lin and Goldstein present a computational model of the auditory periphery that provides an account of the nonlinear input/output characteristics of the cochlea. The major feature of this

model is a *multiple band-pass nonlinearity* (MBPNL) filter bank, which has been tested with a broad range of cochlear responses (e.g., Goldstein, 1995). A program is described that implements a time-domain version of the MBPNL model and runs in an X window environment. The C source code for this program is available from the authors on request. Results of the model are presented, which show level dependence in click responses similar to that observed experimentally in measurements of basilar membrane motion. Cochlear impairments are easily simulated in this model by reducing the "tip gain" associated with tuning in the cochlea.

In the fifth chapter, Kates investigates the use of a cochlear model to develop an adaptive processing strategy for hearing aids. The idea is to use a cochlear model to simulate the output of an impaired ear, then devise a hearing-aid processor that will restore, as much as possible, the normal output of the ear. The weights of an adaptive filter are adjusted to minimize the (mean-squared) difference between the output of the normal ear with unfiltered input and the output of the impaired ear with filtered input. Both time-based (Kates, 1991) and frequency-based approaches are considered for the cochlear model. Each approach has its advantages and disadvantages. An example is described where this processing strategy is used with a speech signal, but the results have not yet been tested with subjects.

Physiological and perceptual models, like the ones described in this section, provide an essential framework for understanding normal and impaired hearing processes. In addition, computational models, based largely on observations of animal models, offer insights into processing strategies that might be used to partially restore normal hearing to an impaired ear.

REFERENCES

Goldstein, J. L. (1995). Relations among compression, suppression, and combination tones in mechanical responses of the basilar membrane: Data and MBPNL model. *Hearing Research, 89*, 52–68.

Jenison, R. L., Greenberg, S., Kluender, K. R., & Rhode, W. S. (1991). A composite model of the auditory periphery for the processing of speech based on the filter response functions of single auditory nerve fibers. *Journal of the Acoustical Society of America, 90*, 773–786.

Kates, J. M. (1991). A time-domain digital cochlear model. *IEEE Transactions on Signal Processing, 39*, 2573–2592.

Schmiedt, R. A., Mills, J. H., & Adams, J. C. (1990). Tuning and suppression in auditory nerve fibers of aged gerbils raised in quiet or noise. *Hearing Research, 45*, 221–236.

Young, E. D., & Barta, P. E. (1986). Rate responses of auditory nerve fibers to tones in noise near masked threshold. *Journal of the Acoustical Society of America, 79*, 426–442.

Young, E. D., & Sachs, M. B. (1979). Representation of steady-state vowels in the temporal aspects of the discharge patterns of populations of nerve fibers. *Journal of the Acoustical Society of America, 66*, 1381–1403.

1

Cochlear Excitation Patterns in Sensorineural Hearing Loss

Eric Javel
Dept. of Otolaryngology
University of Minnesota

A computational model has been developed that simulates neuronal responses of the cat inner ear. The model is based on descriptions of middle ear mechanics, spiral ganglion innervation density, active and passive cochlear mechanics, neural and mechanical input–output functions, rapid and short-term adaptation, neuron-to-neuron variation in response properties, and stochastic response behavior. Its output is the predicted rate response of every fiber in the auditory nerve to arbitrary, user-specified signals. The model has been specifically constructed to allow simulation of various forms of sensorineural or conductive hearing loss. This is achieved by modifying one or more model components in the desired manner; for example, numbers and loci of surviving hair cells. This chapter utilizes the model to demonstrate effects of hearing loss on neural responses to tones and speech, and to examine possible neural mechanisms underlying performance on perceptual tasks.

INTRODUCTION

Research on the anatomy, mechanics, and physiology of the cochlea and auditory nerve has progressed to the point where virtually all aspects of end organ response to sound have been thoroughly characterized. This is true for both normal hearing and some types of sensorineural hearing loss. Middle-ear transfer functions have been studied (Nedzelnitsky,

1980), and cochlear innervation patterns have been described in normal and pathological ears (Leake & Hradek, 1988; Liberman & Kiang, 1984; Spoendlin, 1972). Linear and nonlinear aspects of basilar membrane (BM) mechanics have been described (Rhode, 1971; Ruggero & Rich, 1991), and these have been modeled (Allen, 1980; Geisler, 1991; Neely, 1993). Also, electrical and motile responses of outer and inner hair cells have been characterized (Brownell, Bader, Bertrand, & de Ribaupierre, 1985; Cody & Russell, 1987; Dallos, 1985), and tuning properties and input–output functions of primary afferents have been analyzed in considerable detail (Javel, 1986, 1994; Javel & Farrell, 1995; Kiang, 1965; Liberman & Kiang, 1978; Schmiedt, Zwislocki, & Hamernik, 1980). Finally, synaptically mediated effects such as rapid and short-term adaptation have been studied (Westerman & Smith, 1984), and descriptions of stochastic or random aspects of neural response have been developed (Siebert, 1965; Teich & Khanna, 1985; Young & Barta, 1986).

The relatively complete state of knowledge about cochlear structure and function makes it possible to develop a computer-based model of the entire cochlea and auditory nerve. This chapter describes the development of this model for the cat ear, indicates its responses to tones and speech in normal and impaired hearing, and examines its applicability to the study of neural coding mechanisms underlying perceptual performance.

ELEMENTS OF THE MODEL

Major design objectives of the model were to (a) represent spatial differences in neural innervation pattern correctly; (b) duplicate known distributions of response behaviors, such as spontaneous rate (SR), threshold variation, and so on; (c) generate physiologically accurate renditions of absolute sensitivity, neural tuning properties, suprathreshold response behavior, and correlations among response measures; (d) incorporate mechanisms that result in the same amounts of variation in responses that occur across fibers in laboratory experiments; (e) provide for trial-to-trial variability or stochastic response behavior; and (f) compartmentalize response parameters so that neural activity in various types of hearing impairment could be predicted.

A model cochlea was built in software by moving through the inner ear in steps of one inner hair cell (IHC), generating the number of spiral ganglion cells to be connected to it by randomly sampling the innervation density distribution (Leake & Hradek, 1988), and assigning response parameter values to each cell by randomly sampling distributions that

were appropriate for its characteristic frequency (CF). Parameters included spontaneous rate, threshold at CF, slopes of rate-intensity functions, maximum discharge rate, tuning sharpness, magnitude and time course of adaptation, and so on. This scheme results in parameter distributions that are physiologically correct at each CF and across the entire neural population, and it generates appropriate across-fiber differences in response.

Neural excitation patterns were obtained by specifying a signal, then computing the response of each fiber in the simulated auditory nerve to that signal. Trial-to-trial variability in spike counts for each fiber was achieved by computing and then randomly sampling the Gaussian distribution that describes mean discharge rate and its variance. For complex tones, sound energy passing through a fiber's tuning curve was summed linearly. This formed the input to a transducer function whose output was the net rate response to the signal. Mechanical nonlinearities, such as two-tone suppression and combination tone generation, are not included in the model, but active cochlear processes and synaptically mediated effects are included.

An example of common physiological response measures for a synthesized high-SR fiber tuned to 1 kHz is shown in Fig. 1.1. These were obtained by simulating laboratory data acquisition procedures in software. The fiber's response area (0–90 dB SPL in 10-dB steps) is shown in the upper left panel, its tuning curve is shown at the upper right, a poststimulus time (PST) histogram to a CF tone presented 20 dB above threshold is shown at the lower left, and the rate-intensity function obtained for single presentations of a 200-ms CF tone is shown at the lower right. Except for the lack of a reduction in discharge rate after tone offset (which is not currently implemented in the model), all these responses appear realistic.

Examples of random variation in tuning properties and input–output functions are shown in Fig. 1.2. On the left are overlaid tuning curves of all fibers innervating a single IHC tuned to 2 kHz, and on the right are shown these fibers' rate-intensity functions to CF tones. Responses of high-SR fibers (SR $\geq$ 18 spikes/s) are plotted with solid lines; medium-SR fibers (0.5 $<$ SR $<$ 18), with long dashed lines; and low-SR fibers (SR $\leq$ 0.5), with short dashed lines. The shapes of the tuning curves and rate-intensity functions are correct, as are the relationships of threshold to SR and maximum discharge rate, and the degree of response variation across fibers.

Figure 1.3 shows thresholds of every 10th fiber in the model ear, plotted as a function of each fiber's CF. Like Liberman's (1978) data, low-SR fibers exhibit a variety of thresholds that span a 40-dB range, whereas medium-SR fibers and high-SR fibers tend to cluster near absolute threshold.

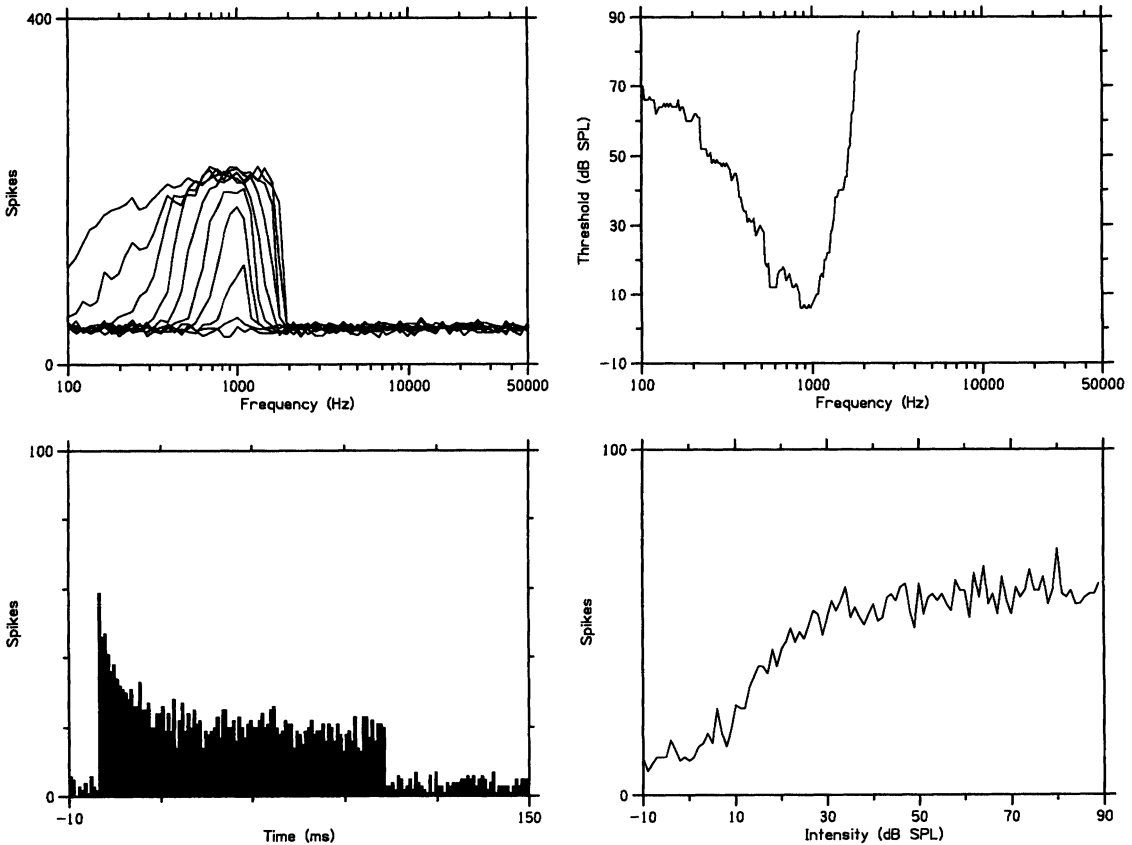

FIG. 1.1. Response area (upper left), tuning curve (upper right), PST histogram (lower left), and rate-intensity function at CF (lower right) for a synthesized auditory nerve fiber tuned to 1 kHz.

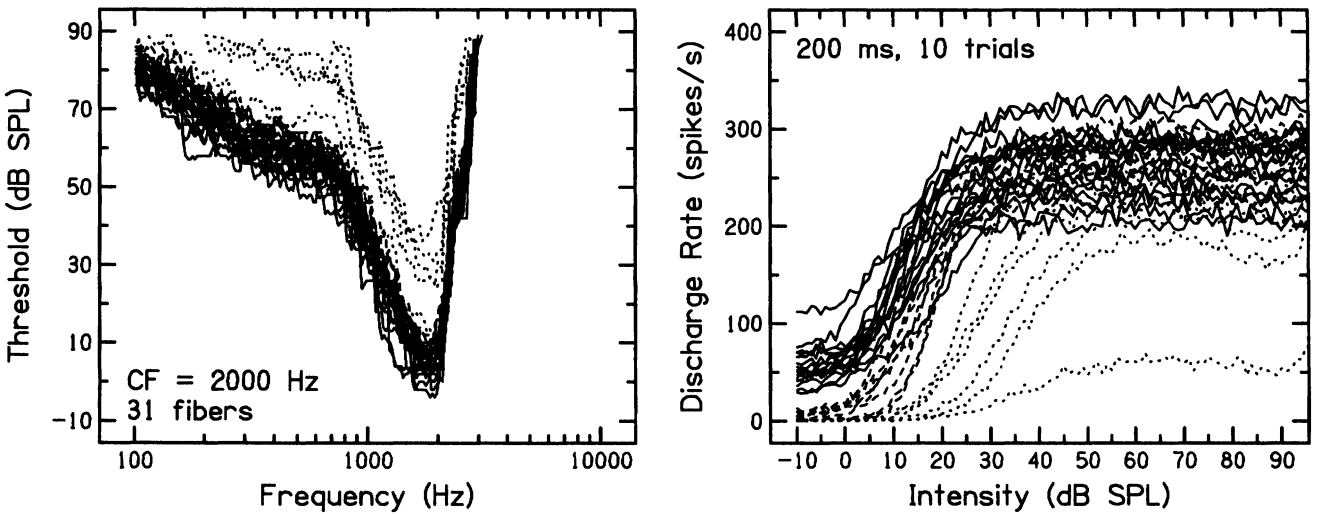

FIG. 1.2. Tuning curves (left) and rate-intensity functions at CF (right) for all fibers connected to a single IHC tuned to 2 kHz. Solid lines indicate responses of high-SR fibers, long dashed lines indicate responses of medium-SR fibers, and short dotted lines indicate responses of low-SR fibers.

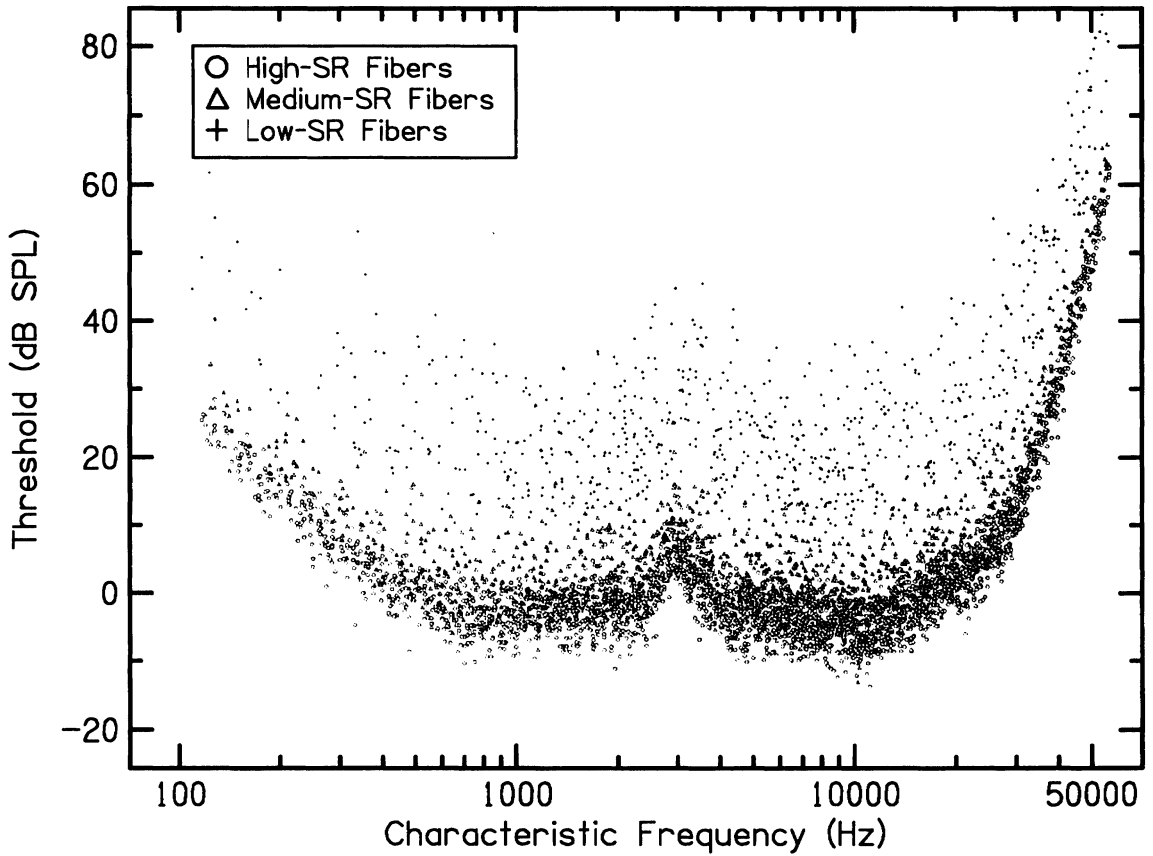

FIG. 1.3. Thresholds of every 10th fiber in the model ear, plotted as a function of each fiber's CF. Different symbols indicate fibers from each of the three SR classes.

POPULATION RESPONSES IN NORMAL EARS

Neural population responses to 100-ms pure tones at various frequencies and a level of 40 dB above behavioral threshold (normal hearing level, nHL) are shown two ways in Fig. 1.4. The responses shown on the left are total spike counts of every 10th fiber in the synthesized nerve, plotted as a function of the fiber's location along the cochlear duct. Each dot represents the response of one fiber, and the population response at each intensity contains data from 5,150 fibers. Driven activity is observable as counts extending above a background of spontaneous activity. The righthand column in Fig. 1.4 shows the summed driven responses of all fibers connected to each IHC, plotted as a function of IHC locus. Driven activity is defined as that evoked by the signal, minus a sample of SR for an equal duration. Each point in this case represents the output of one IHC.

Similar to the tuning properties of single auditory nerve fibers, the spatial extent of the population response is inversely related to frequency. Also observable is the log-linear relationship of signal frequency to place of maximal activity at high frequencies and the compressed representation of low frequencies in the apical portion of the cochlea (Liberman, 1982). Displays such as these provide a foundation for understanding the spatial distribution of neural responses in normal ears and serve as a springboard for analyzing neural activity in impaired hearing.

HEARING IMPAIRMENT

Hearing loss may arise from more than one source. In addition to simple attenuative effects produced by conductive deficits mediated by middle ear structures, threshold shifts and modified suprathreshold responses may also arise from OHC dysfunction or loss, IHC loss, or from reduction in endocochlear potential (which drives both OHCs and IHCs). Impairment in the model is specified by files describing spatial distributions of degree of OHC function, the presence or absence of IHCs, and/or amount of endocochlear potential (EP) reduction. Decreased OHC function produces changes in tuning properties and suprathreshold response behavior by reducing the gain of the "cochlear amplifier." The approach employed here is similar to the one described by Neely (1993). It is assumed that active gain magnitude is linearly related to the number of functional OHCs at each cochlear locus, which in turn affects the micromechanics of the affected IHCs.

EP dysfunction occurs in furosemide intoxication (Ruggero & Rich, 1991; Sewell, 1984) and in Meniere's disease or endolymphatic hydrops. It is assumed here that reduced EP magnitude linearly translates into

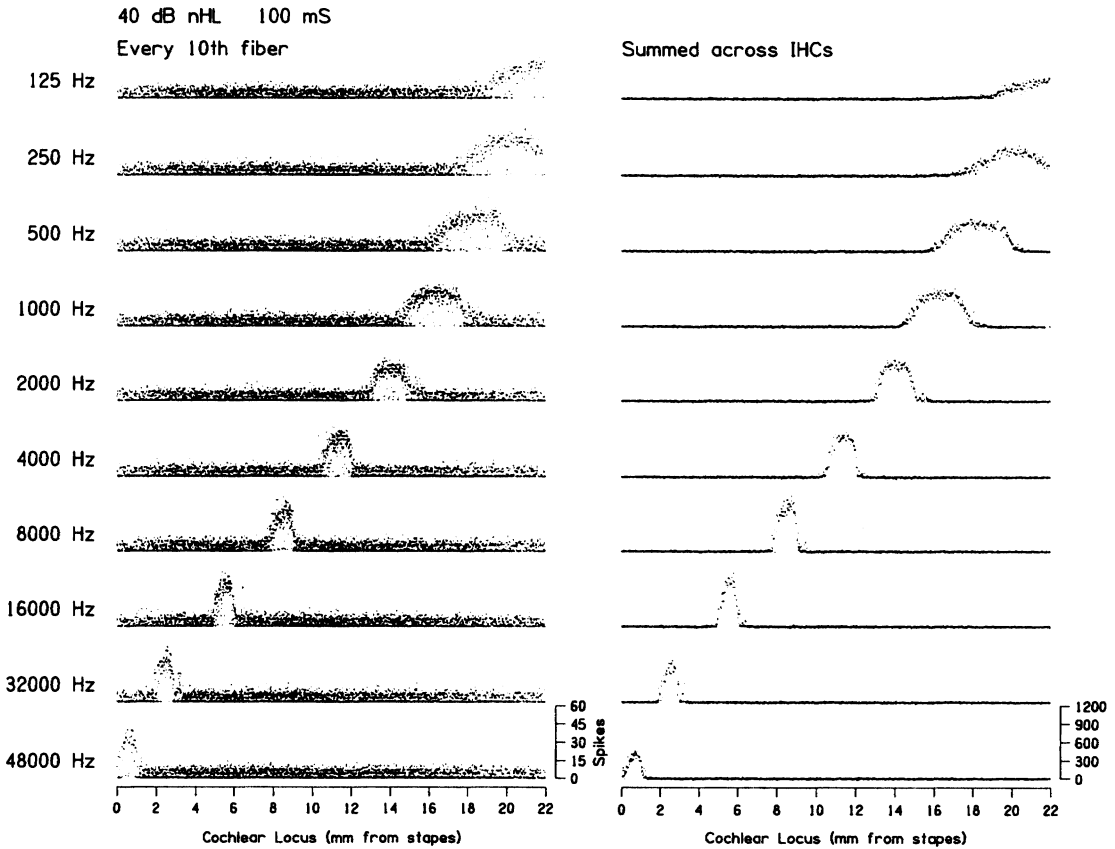

FIG. 1.4. Neural population responses in the normal ear to 100-ms tones presented at 40 dB nHL and at the indicated frequencies. On the left are shown responses of every 10th fiber in the nerve, and on the right are shown the summed responses of all fibers connected to each IHC.

reduced motility of OHCs (hence altered tuning and suprathreshold response properties) and reduced SRs and maximum discharge rates in fibers connected to IHCs.

Figure 1.5 shows the progression of degraded tuning of individual fibers in the model as OHC loss increases (and cochlear amplifier gain decreases). The tuning curves shown are of high-SR fibers with "average" response characteristics with unimpaired CFs of 0.5, 2, and 8 kHz. As OHC function declines, tuning curve "tips" become truncated as CF shifts downward (Liberman & Kiang, 1978), and "tails" become hypersensitive (Schmiedt et al., 1980). Sensitivity loss is proportionately greater at higher CFs than at lower CFs, because the gain of the cochlear amplifier increases with CF (Neely, 1993).

Neural population responses to 1 kHz tones across intensity are shown in Fig. 1.6 for the normal ear and for the same ear but with 50% and 100% OHC impairment uniformly applied throughout the cochlea. Although not particularly realistic in a clinical sense, these impairments have been selected to demonstrate the effects of progressive detuning on neural excitation patterns. Responses have been summed across all fibers innervating each IHC. Activity is restricted to a fairly narrow spatial extent at low intensities, and the spatial distribution expands basally at

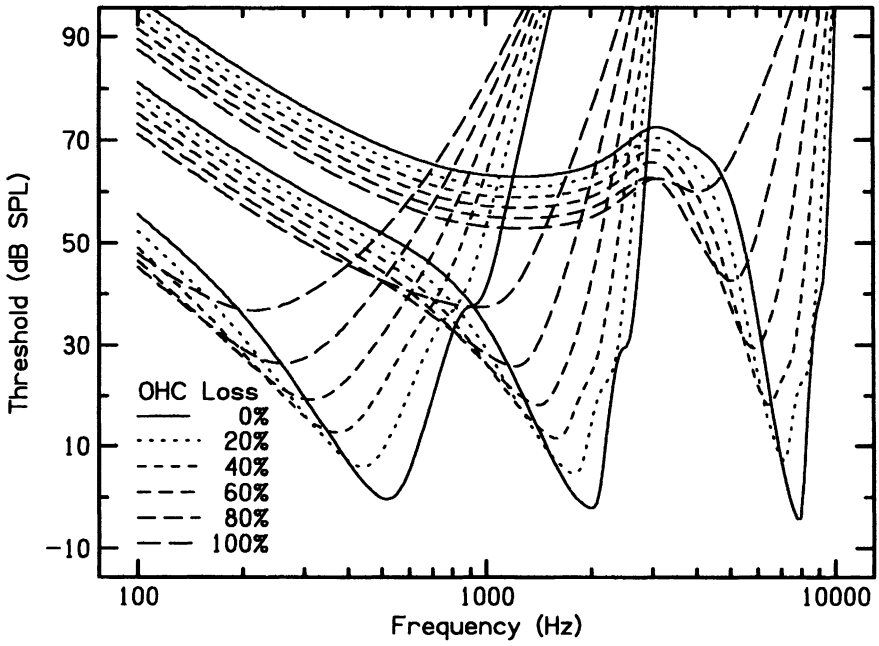

FIG. 1.5. Changes in tuning curve shape as OHC loss progressively increases.

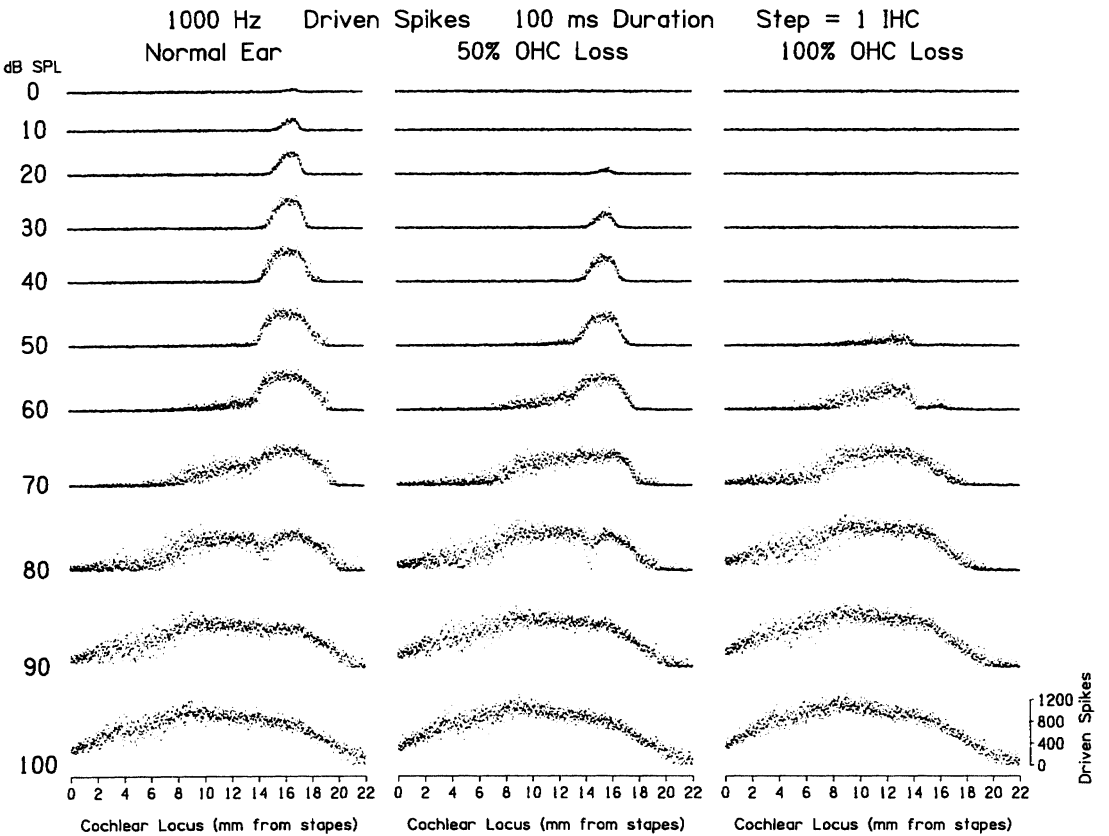

FIG. 1.6. Neural population responses to 1 kHz as a function of level in the normal ear (left) and in the same ear but with 50% OHC dysfunction (center) and 100% OHC dysfunction (right).

high intensities. The dip in response near the 14-mm locus at 90 dB SPL in the normal ear occurs because these fibers exhibit nonmonotonic rate-intensity functions, for which the model accounts. A threshold shift of about 20 dB occurs at 1 kHz when OHC function is 50% impaired, and the shift is 40–50 dB for 100% impairment. The width of the excitation pattern at near-threshold intensities varies directly with the amount of OHC dysfunction, and the spatial locus of the excitation pattern peak shifts basally as OHCs become progressively more impaired. However, the intensity at which responses start spreading basally does not change with increasing OHC impairment, and by 100 dB SPL the excitation patterns for both normal and pathological conditions are similar in magnitude and spatial extent.

Distributions of OHC, IHC, and EP function for 50% and 100% OHC loss and two other manipulations to be described later are shown in Fig. 1.7, and the corresponding "audiograms" are shown in Fig. 1.8. The latter were obtained by determining the lowest intensities at which neural population responses exhibit a visually detectable increase in activity. An OHC impairment of 50% produces a mild, slightly sloping loss, and impairment of 100% produces a moderate loss whose configuration is reminiscent of severe presbyacusis.

NEURAL CORRELATES OF PERCEPTUAL PROCESSES

The excitation pattern model was used to examine possible neural correlates of some auditory perceptual processes. The results of an analysis that relates to loudness growth in normal and impaired hearing are shown in Fig. 1.9. Symbols connected by dashed lines indicate driven spike counts obtained across intensity at three frequencies and in two cases of OHC dysfunction. These are referred to the *left-hand axis*. Of interest is the observation that the total counts elicited at low intensities are nearly identical at all three frequencies, although the underlying excitation patterns have different shapes (cf. Fig. 1.4).

The solid line in Fig. 1.9 indicates loudness growth at 1 kHz in human listeners. These data were obtained by Hellman and Zwislocki (1963), and they are referenced to the right-hand axis. Interestingly, the growth in spike counts across intensity undergoes the same change in slope that is observed perceptually at about 20 dB sensation level (SL). This suggests that loudness correlates with the total count elicited in the active neural population, not the amount of activity within a frequency channel or critical band. However, slopes are different for neural response growth and perceptual loudness growth (i.e., 0.19 vs. 0.30). This suggests that an unspecified central mechanism exists which amplifies spike counts before

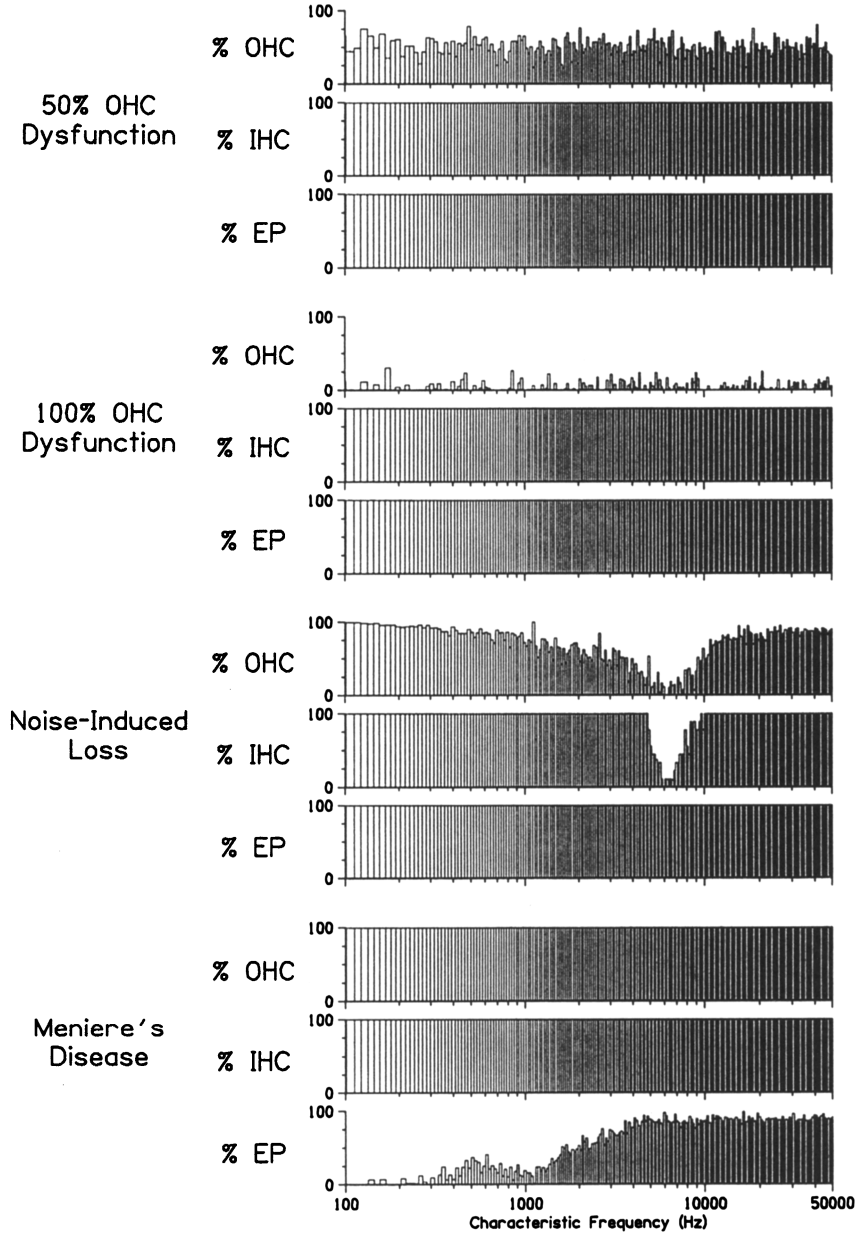

FIG. 1.7. Distributions of relative amounts of OHC function, IHC function, and endocochlear potential (EP) for hearing losses described in this chapter, plotted as a function of frequency.

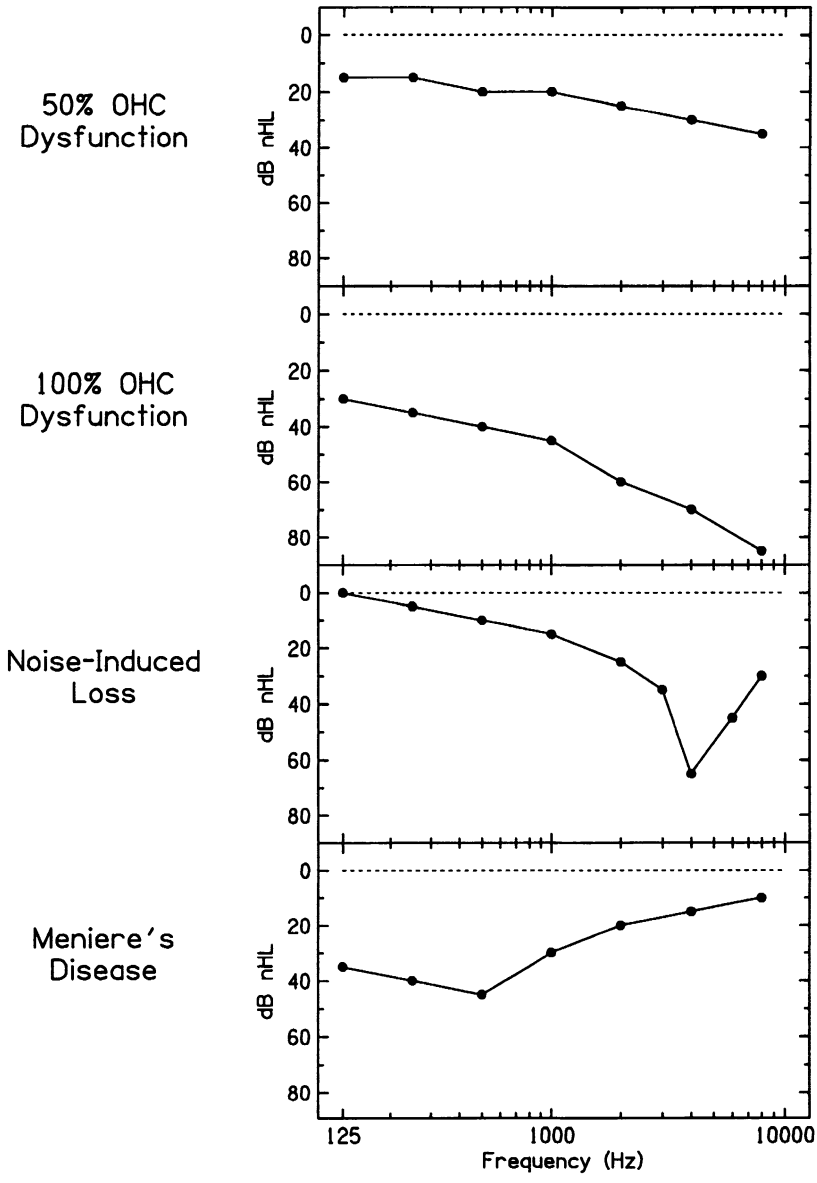

FIG. 1.8. "Audiograms" for various types of hearing impairment, obtained from visual inspection of excitation patterns.

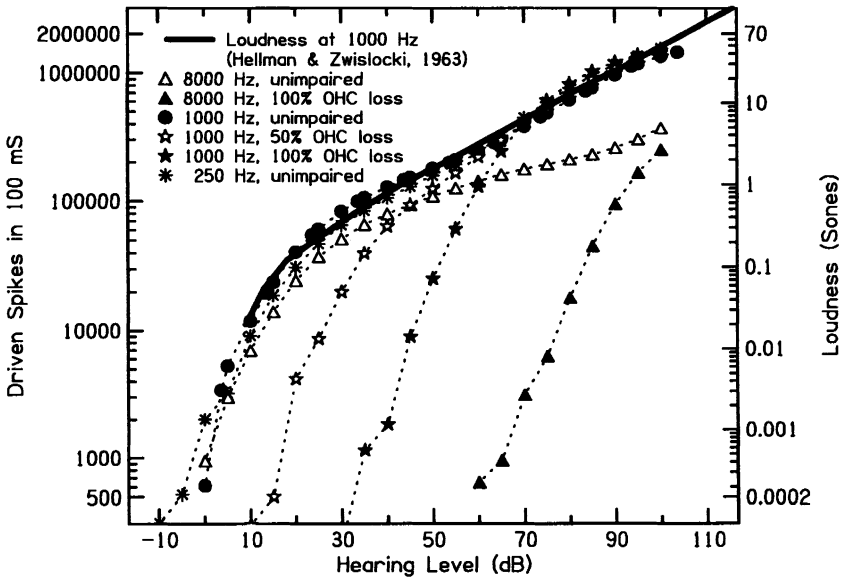

FIG. 1.9. Correlates of loudness growth and recruitment. The excitation pattern model anticipates the change in slope of loudness growth in normal ears and provides an explanation for loudness recruitment in cochlear hearing loss.

loudness is assigned, that growth of spike counts across intensity differ between humans and cats, or that certain model parameters are incorrect.

A possible neural correlate of loudness recruitment exists in the spike count data obtained for 50% and 100% OHC loss. Consider the data at 1 kHz, indicated by stars and filled circles. 100% OHC loss produces a threshold shift of about 35 dB. Spike counts at audible levels (>35 dB nHL) grow at the same rate as in the normal ear, but the threshold shift causes counts to continue growing until they approach those obtained when no impairment exists. The slope and counts then change to the same values as in normal hearing. If a 1 kHz tone in the impaired ear becomes audible at 35 dB nHL and elicits the same number of spikes at 70 dB nHL as in the normal ear, and if loudness is related to total spike counts, then by 70 dB nHL the tones must be equally loud. Although counts in the impaired ear increase at the same rate as at low levels in the normal ear, loudness must be growing abnormally rapidly in the impaired ear because the rate of growth of spike counts is greater in the impaired ear than in the normal ear at most SLs. Continuing this line of reasoning, loudness recruitment would end when counts in the impaired ear intersect counts in normal hearing. For 100% OHC loss at 1 kHz, this would occur at 65–70 dB nHL.

The model predicts that a pure OHC loss would have different effects on neural counts across intensity (and hence on loudness growth) than would a pure IHC loss. The major effects of OHC loss are to create a threshold shift and a corresponding increase in the intensity at which driven spike counts undergo a slope change. For example, in Fig. 1.9 total OHC loss causes the inflection to shift from 20 dB nHL to 70 dB nHL for a stimulus frequency of 1 kHz. A less-than-total OHC loss would cause the inflection to occur at an intensity between 20 and 70 dB nHL. Thus, OHC loss causes a portion of the neural response growth curve to shift *horizontally*. Although the amount of OHC loss controls the intensity at which the inflection occurs, response growth rates at intensities above and below the inflection point do not change substantially. Perceptually, changes in the inflection point would be manifested as threshold shifts and differences in the intensity range over which loudness recruitment occurs.

In contrast, a pure IHC loss reduces the total spike count without affecting the position of the inflection point along the intensity axis. This happens because removing an IHC eliminates activity in all the fibers connected to it without altering active mechanical processes. Thus, uniform IHC loss causes the entire neural response growth curve to shift *vertically*. This approach predicts that IHC loss will produce decreased loudness at a fixed intensity but no recruitment. Clinically, the most common situation would likely involve place-dependent losses of both OHCs and IHCs. Therefore, predicting specific patterns of loudness recruitment in these individuals involves applying both horizontal and vertical shifts of the neural growth rate function.

A second demonstration of the excitation pattern model's ability to account for perceptual findings is tone-on-tone masking or psychophysical tuning curves. These were generated for simultaneous masking conditions by first determining the spatial extent of activity and spike count elicited by a fixed-frequency, fixed-intensity probe, then determining the intensities at which different-frequency maskers elicited the same number of spikes in the active subpopulation as the probe. Plotting masker level as a function of masker frequency provides a neural correlate of psychophysical tuning curves.

Examples are shown in Fig. 1.10 for a model cat ear with normal hearing and with 100% OHC loss, for probes at 0.25, 1, and 8 kHz. Probe level was varied in 10-dB steps from 5 dB SL to 55 dB SL. As probe level increases, the masking patterns become shallower, with the "tips" of the tuning curves usually changing more rapidly than the tails in the normal ear and at about the same rate in the impaired ear. Taken another way, the slope of the masking function is >1 for maskers below probes ≥ 1 kHz, and it is very close to 1 for masker frequencies near the probe in normal ears, and at all

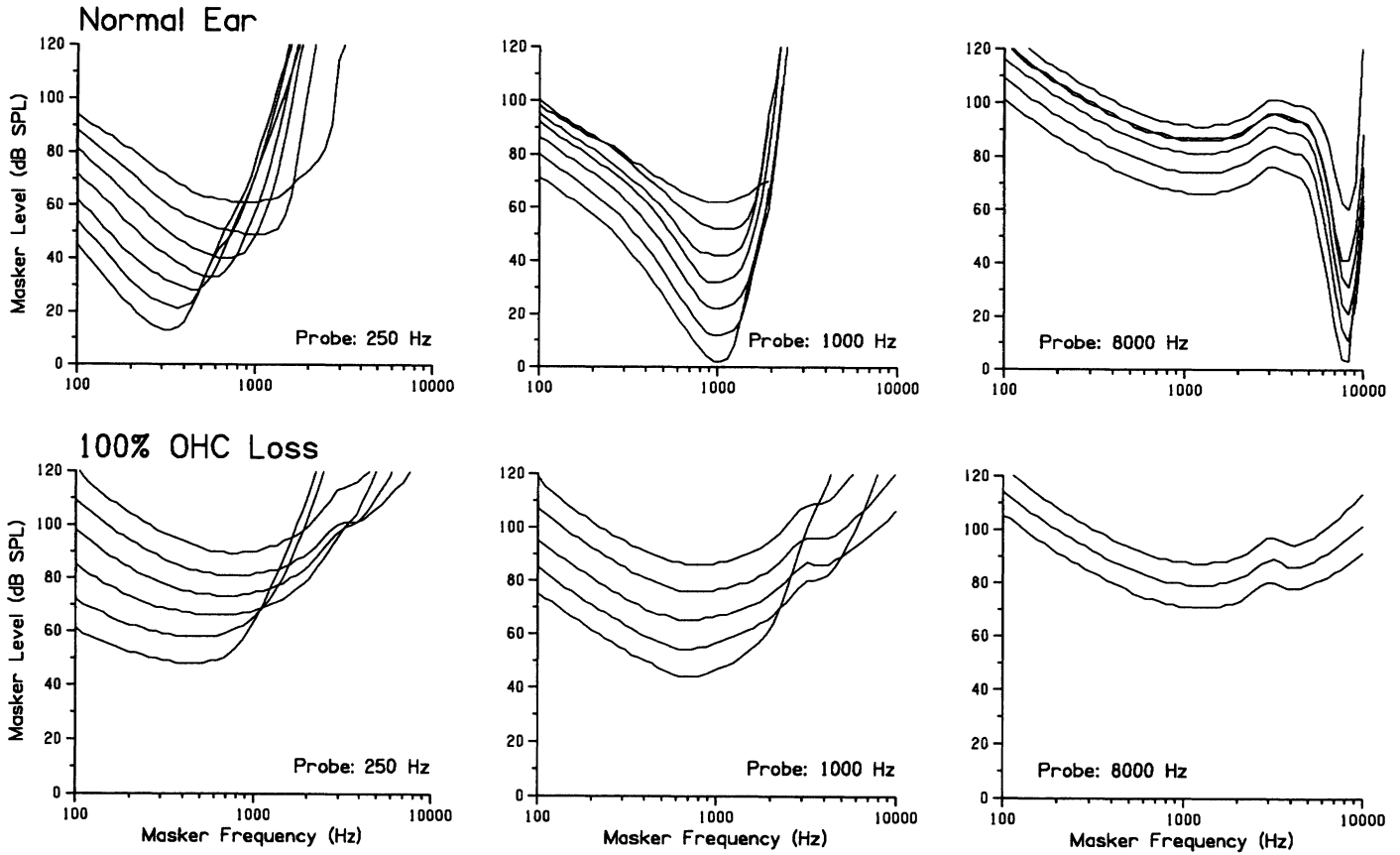

FIG. 1.10. Excitation pattern model correlates of psychophysical tuning curves in normal hearing and with 100% OHC impairment. The lowest probe levels are 5 dB SL, increasing in 10-dB steps.

frequencies when substantial OHC impairment exists. Also, impairment reduces the slope of the high-frequency side of the psychophysical tuning curve. All these findings have previously been described in perceptual studies (Carney & Nelson, 1983; Zwicker & Schorn, 1978). An important aspect of these data is that the increased rate of masking growth at low frequencies in normal ears is *not* due to increased slopes of rate-intensity functions in individual fibers at these frequencies. Rather, the slope of the masking function exceeds unity because excitation patterns for low-frequency maskers spread basally at rapid rates as intensity increases. When enough hearing impairment exists, the rapid growth of masking caused by basalward expansion of the excitation pattern is counteracted by the fact that the spatial extent of activity elicited by the probe already contains the expansion. This leads to masking growth rates that are nearly linear.

RESPONSES TO SPEECH

Sachs and Young (1979) described neural population responses to the vowel /eh/ presented in isolation. They determined that formants were individually represented in spatial distributions of neural activity only at low intensities, and that representations of formants as spatially distinct peaks of activity were maintained over a wider range of intensities in responses of low-SR fibers than in high-SR fibers. They hypothesized that the perceptual system could encode formants by place of activation over a wide intensity range if responses of low-SR fibers could be selectively monitored at higher intensities.

The excitation pattern model was used to examine responses to speech by determining responses of selected subsets of the fiber population and by computing responses under various conditions of hearing impairment. The signal used was the same steady-state vowel /eh/ described by Sachs and Young, and it was presented to the model for the same 400-ms duration. The vowel spectrum is shown in Fig. 1.11.

Responses to /eh/ in the normal ear and in ears with 50% and 100% OHC loss are shown as a function of overall level in Fig. 1.12. Driven spike counts have been summed across IHCs and plotted as a function of CF (rather than cochlear locus) to simplify comparisons with the vowel spectrum. Similar to Sachs and Young's findings, spatially distinct responses to the first formant (512 Hz) and to the second/third formant complex are observable at low levels in the normal ear. These responses saturate at about 49 dB. The troughs between the formant peaks fill in at higher levels, and spatial representation of formants is lost. Reducing OHC function by 50% leads to generally similar findings, except that the representation of the higher-frequency formants is poorer because 50%

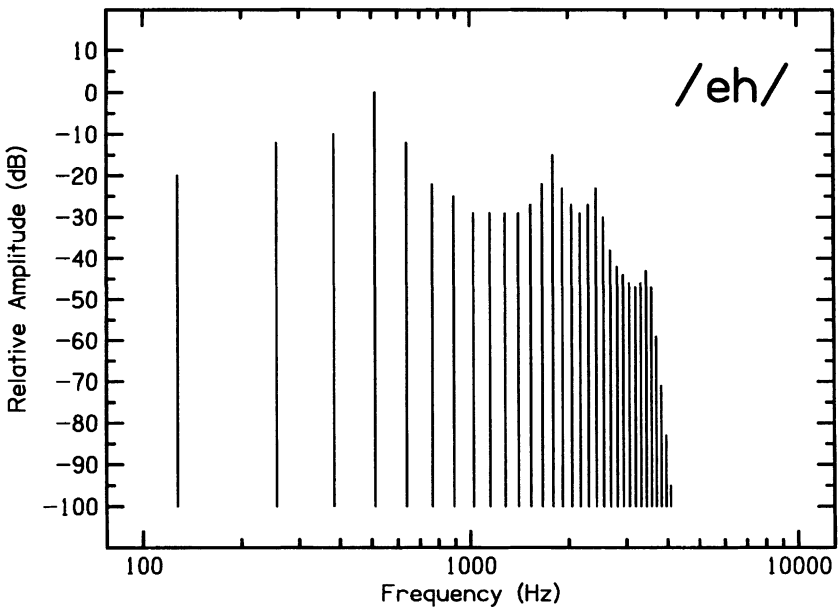

FIG. 1.11. Spectrum of the vowel /eh/ used by Sachs and Young (1979) and in the present study.

reduction in function produces a greater threshold shift at higher frequencies than at low frequencies. Eliminating OHC function produces a larger change. In addition to a threshold shift, the representation of the second and third formants is almost entirely lost, and the only obvious response is to the first formant. Also, activity is maximal in fibers originally possessing CFs higher than the formant frequencies. This is not surprising, given the fact that OHC loss causes neural responses to become driven by passive BM mechanics, which peak at a more basal position and lead to lower fiber CFs (cf. Fig. 1.5).

As alluded to earlier, the modular structure of the excitation pattern model makes it possible to examine responses in fiber subsets and to simulate particular sensorineural hearing losses. Two such demonstrations shown here are responses to /eh/ of low-SR fibers (Fig. 1.13) and responses in noise-induced hearing loss (NIHL) and Meniere's disease (Fig. 1.14).

Consistent with Sachs and Young's (1979) findings, spatial representation of formant frequency in the normal ear is maintained at higher intensities in responses of low-SR fibers (Fig. 1.13, left column). However, at high intensities some spatial distinctness is lost even for low-SR fibers. Reducing OHC function by 50% (Fig. 1.13, center) and 100% (Fig. 1.13, right) introduced threshold shifts, as seen earlier, and it caused responses of

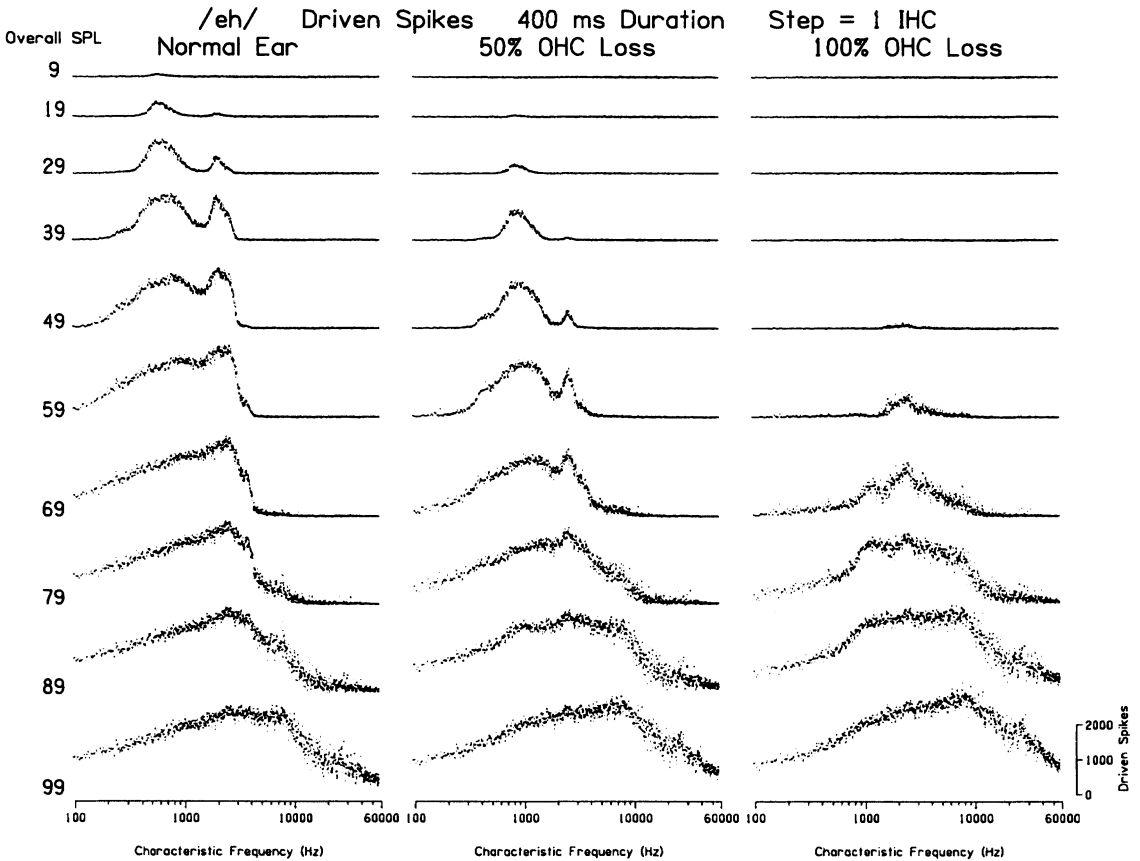

FIG. 1.12. Responses of the excitation pattern model to /eh/ as a function of level for the unimpaired ear (left) and with 50% (center) and 100% (right) OHC loss.

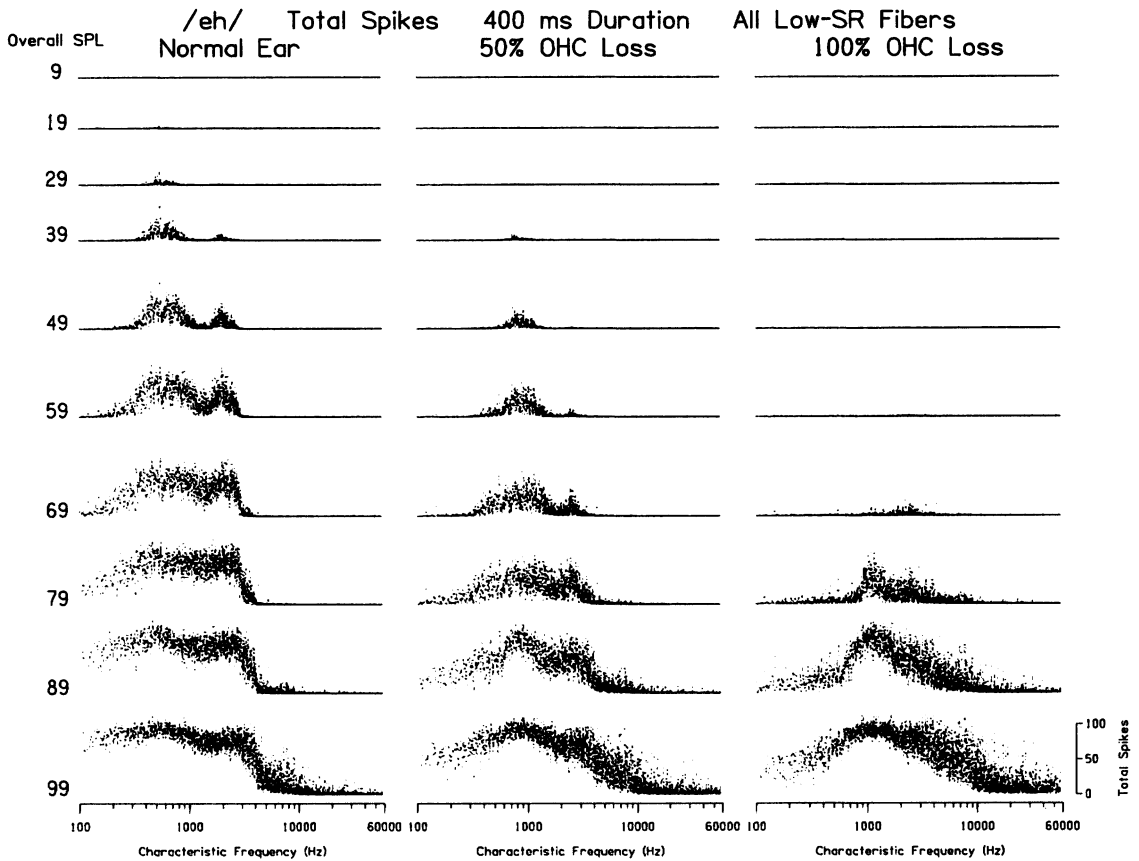

FIG. 1.13. Responses to /eh/ of all low-SR fibers in the simulated cochlea as a function of level, in the normal hearing condition (left) and in conditions of 50% (center) and 100% (right) OHC loss.

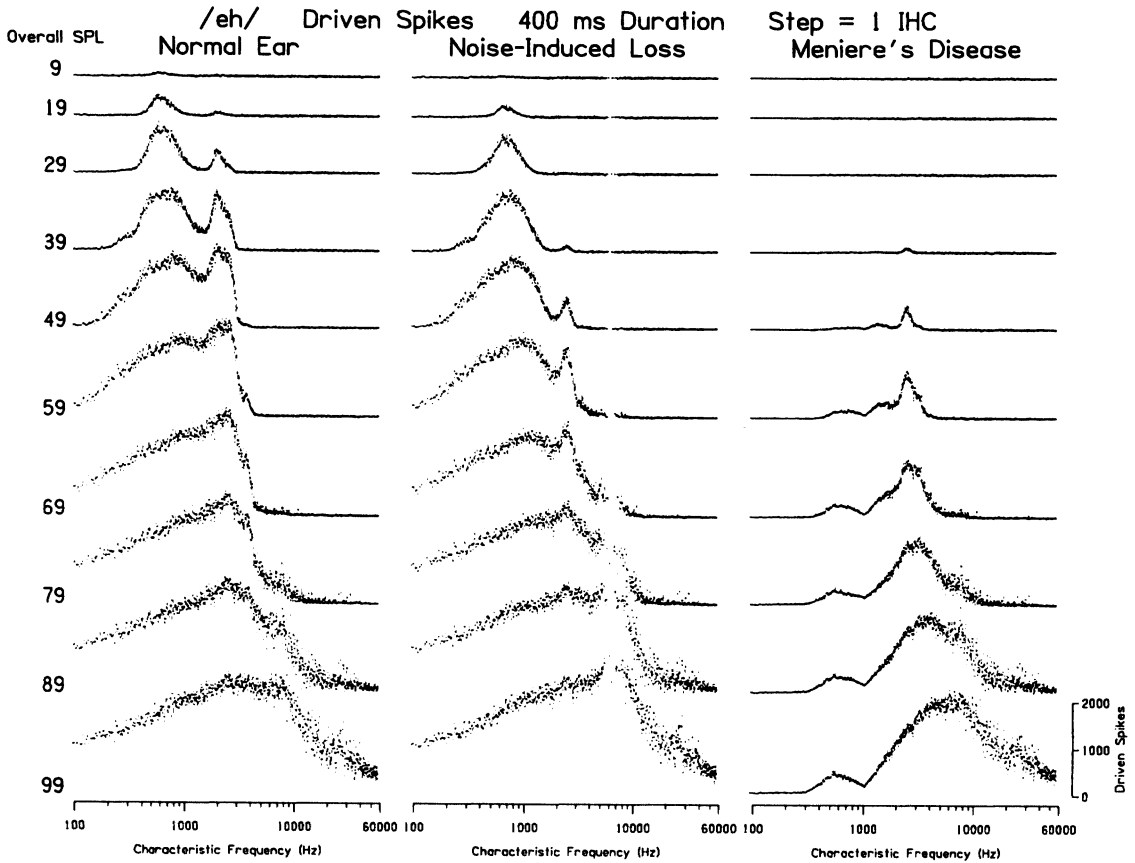

FIG. 1.14. Responses of the excitation pattern model to /eh/ as a function of level under conditions of simulated noise-induced hearing loss (center) and Meniere's disease (right). Responses of the unimpaired ear are shown at the left for reference purposes.

low-SR fibers to undergo some unusual modifications across frequency. OHC loss caused a basalward shift in the locus of responsive fibers (i.e., toward higher CFs), but the level at which excitation patterns start expanding basally did not change. This, in turn, caused low-SR fibers to lose spatial specificity at a lower intensity, relative to threshold, than occurs normally.

Responses to /eh/ of ears with NIHL and Meniere's disease are shown in Fig. 1.14. Responses of the unimpaired ear are shown at the left for reference purposes. As depicted earlier in Fig. 1.7, NIHL was simulated by eliminating some IHCs tuned near 6 kHz and by decreasing OHC function to 0% in a broad manner with a minimum at the 6 kHz locus. In accord with the well-documented half-octave difference between site of lesion and the frequency affected most severely, maximum threshold shift occurred at 4 kHz. The corresponding "audiogram" was shown earlier in Fig. 1.8. IHC loss in the NIHL condition leads to no responses from the fibers connected to them (observable as a lack of activity at CFs near 6 kHz). The loss of OHC function in the middle cochlear turn leads to degraded spatial representation of the higher formants but essentially no change in the internal representation of the first formant (because OHC function is normal in this region).

Meniere's disease (or more appropriately, endolymphatic hydrops) was simulated by progressively reducing EP in the middle and apical cochlear turns to 0 mV while leaving IHCs and OHCs intact. As noted earlier, EP loss produces concomitant reductions in both OHC and IHC function and can lead to greatly lowered SRs and maximum discharge rates. This configuration produced the upward-sloping "audiogram" shown in Fig. 1.8.

The responses of the hydropic ear to /eh/ (Fig. 1.14, right column) are vastly different from any of the previously described conditions. Only a single peak emerges at near-threshold levels, and it stems from fibers originally tuned to frequencies around 4 kHz. Analysis of the proportions of the overall response due to each vowel formant (not shown) indicated that the internal representation of the first formant is lost at all but high levels and that the response is primarily to the second and third formants.

As a final demonstration of ways the excitation pattern model may be used, the ears with NIHL and Meniere's disease were fitted with "virtual hearing aids." This was achieved in the simplest way, namely by applying frequency-dependent gain to the input signal in a manner that mirrored the hearing losses shown in Fig. 1.8. More elaborate amplification techniques, multichannel compression for example, may also be investigated with relative ease.

Responses of the impaired model ears to spectrally compensated /eh/s at 40 dB SL are shown in Fig. 1.15. Selective amplification of high frequencies improves the internal representation of the second and third

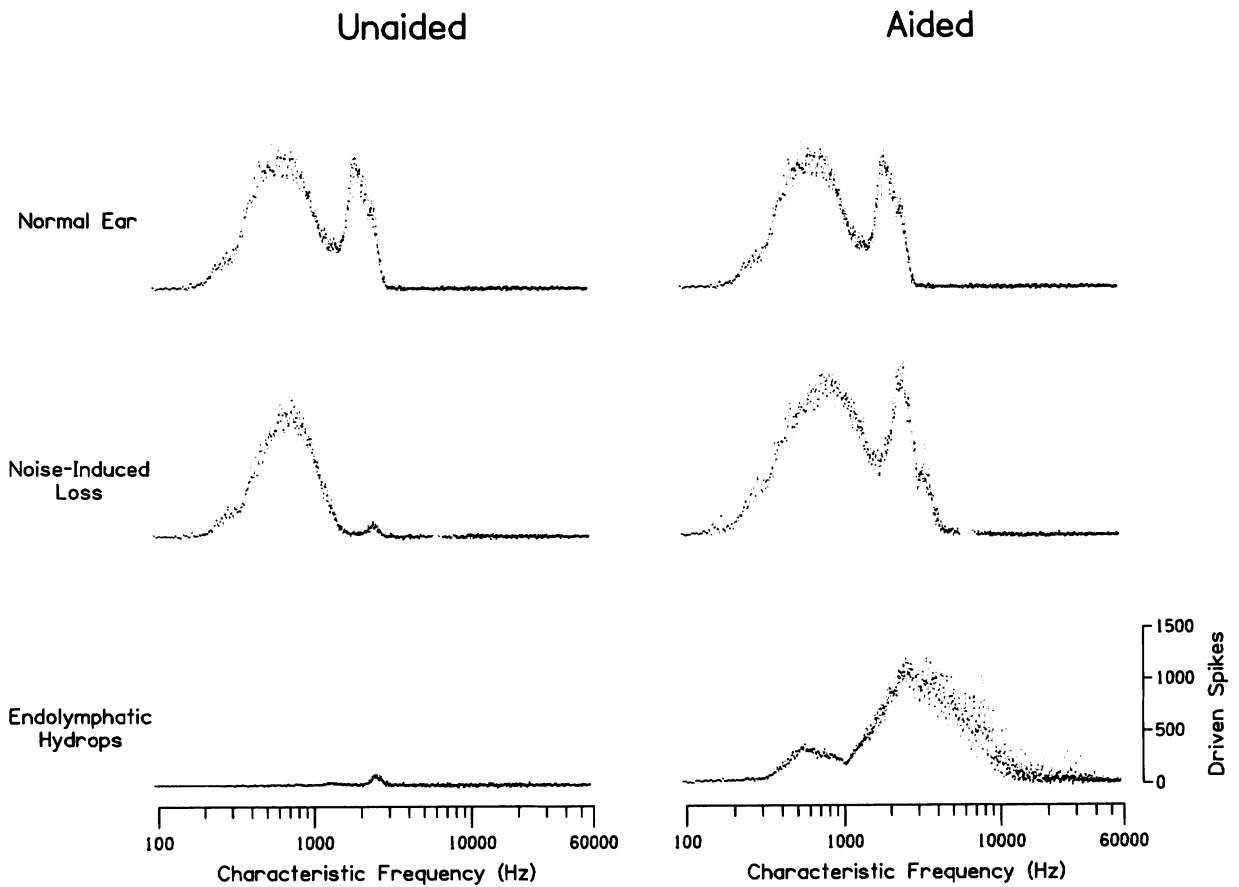

FIG. 1.15. Responses of normal and impaired ears to /eh/ presented at 40 dB SL. Signal spectra for the impaired ears were adjusted to compensate for the hearing loss.

formants in the NIHL ear, but not quite to normal levels. In contrast, providing relatively large amounts of low-frequency emphasis to the ear with Meniere's disease does little to improve the situation. This is because EP loss causes IHCs in the apical cochlear turn to become essentially unresponsive. How this type of impairment may be offset using conventional means is not clear.

DISCUSSION

Strengths of the excitation pattern model are the accurate descriptions of cochlear response properties, the inclusion of physiologically realistic measures of fiber-to-fiber response variation, the ability to describe the activity of every auditory nerve fiber, the incorporation of stochastic response behavior, and the opportunities for creating various cochlear lesions and studying their effects. In addition to providing visual displays of the internal representation of acoustic signals in normal and pathological ears, the model may also be used to analyze the ability of user-defined neural coding strategies to account for perceptual performance. Also, it is extendible to other species, including humans.

Weaknesses of the model as it currently exists are the lack of accurate descriptions of the effects of EP loss, inadequate detail about the across-frequency behavior of the active process or "cochlear amplifier," insensitivity to temporal stimulus waveform and neural response properties, and the absence of descriptions of nonlinearities such as two-tone suppression and combination tone generation. The first two weaknesses may be rectified as knowledge about cochlear physiology progresses. The latter two weaknesses could be corrected using existing knowledge; however, doing so would greatly increase the number of calculations needed to create an excitation pattern, making the model computationally unwieldy.

ACKNOWLEDGMENT

This work was supported by research grant number R01 DC 00138 from the National Institute on Deafness and Other Communication Disorders, National Institutes of Health.

REFERENCES

Allen, J. B. (1980). Cochlear micromechanics—a physical model of transduction. *Journal of the Acoustical Society of America, 68,* 1660–1670.

Brownell, W. E., Bader, C. R., Bertrand, D., & de Ribaupierre, Y. (1985). Evoked mechanical responses of isolated cochlear outer hair cells. *Science, 227,* 194–196.

Carney, A. E., & Nelson, D. A. (1983). An analysis of psychophysical tuning curves in normal and pathological ears. *Journal of the Acoustical Society of America, 73,* 268–278.

Cody, A. R., & Russell, I. J. (1987). Guinea pig hair cell responses. *Journal of Physiology (London), 383,* 551–569.

Dallos, P. (1985). Response characteristics of mammalian cochlear hair cells. *Journal of Neuroscience, 5,* 1591–1608.

Geisler, C. D. (1991). A cochlear model using feedback from motile outer hair cells. *Hearing Research, 54,* 105–117.

Hellman, R. P., & Zwislocki, J. (1963). Monaural loudness function of a 1000-cps tone and interaural summation. *Journal of the Acoustical Society of America, 35,* 856–865.

Javel, E. (1986). Basic response properties of auditory nerve fibers. In R. A. Altschuler, R. P. Bobbin, & D. P. Hoffman (Eds.), *Neurobiology of hearing: The cochlea* (pp. 213–246). New York: Raven.

Javel, E. (1994). Shapes of cat auditory nerve fiber tuning curves. *Hearing Research, 81,* 107–126.

Javel, E., & Farrell, B. F. (1995). Dual-phase model of cochlear excitation. *Abstracts Association for Research in Otolaryngology, 18,* 116.

Kiang, N. Y.-S. (1965). *Discharge patterns of single fibers in the cat's auditory nerve.* Cambridge, MA: MIT Research Monograph No. 35.

Leake, P. A., & Hradek, G. T. (1988). Cochlear pathology of long term neomycin induced deafness in cats. *Hearing Research, 33,* 11–34.

Liberman, M. C. (1978). Auditory-nerve response from cats raised in a low-noise chamber. *Journal of the Acoustical Society of America, 63,* 442–455.

Liberman, M. C. (1982). The cochlear frequency map for the cat: Labeling auditory-nerve fibers of known characteristic frequency. *Journal of the Acoustical Society of America, 72,* 1441–1449.

Liberman, M. C., & Kiang, N. Y.-S. (1978). Acoustic trauma in cats: Cochlear pathology and auditory-nerve activity. *Acta Otolaryngologica Supplement, 358,* 1–63.

Liberman, M. C., & Kiang, N. Y.-S. (1984). Single-neuron labeling and chronic cochlear pathology. IV. Stereocilia damage and alterations in rate- and phase-level functions. *Hearing Research, 16,* 75–90.

Nedzelnitsky, V. (1980). Sound pressures in the basal turn of the cat cochlea. *Journal of the Acoustical Society of America, 68,* 1676–1689.

Neely, S. T. (1993). A model of cochlear mechanics with outer hair cell motility. *Journal of the Acoustical Society of America, 94,* 137–146.

Rhode, W. S. (1971). Observations of the vibrations of the BM in squirrel monkeys using the Mossbauer technique. *Journal of the Acoustical Society of America, 49,* 1218–1231.

Ruggero, M. A., & Rich, N. C. (1991). Furosemide alters organ of Corti mechanics: Evidence for feedback of outer hair cells upon the basilar membrane. *Journal of Neuroscience, 11,* 1057–1067.

Sachs, M. B., & Young, E. D. (1979). Encoding of steady-state vowels in the auditory nerve: Representation in terms of discharge rate. *Journal of the Acoustical Society of America, 66,* 470–479.

Schmiedt, R. A., Zwislocki, J. J., & Hamernik, R. P. (1980). Effects of hair cell lesions on responses of cochlear nerve fibers. I. Lesions, tuning curves, two-tone inhibition, and responses to trapezoidal-wave patterns. *Journal of Neurophysiology, 43,* 1367–1389.

Sewell, W. F. (1984). The effects of furosemide on the endocochlear potential and auditory-nerve fiber tuning curves in cats. *Hearing Research, 14,* 305–314.

Siebert, M. W. (1965). Some implications of the stochastic behavior of primary auditory neurons. *Kybernetic, 2,* 206–215.

Spoendlin, H. (1972). Innervation densities of the cochlea. *Acta Otolaryngologica, 73,* 235–248.
Teich, M. C., & Khanna, S. M. (1985). Pulse-number distribution for the neural spike train in the cat's auditory nerve. *Journal of the Acoustical Society of America, 77,* 1110–1128.
Westerman, L. A., & Smith, R. L. (1984). Rapid and short term adaptation in auditory-nerve responses. *Hearing Research, 15,* 249–260.
Young, E. D., & Barta, P. E. (1986). Rate responses of auditory nerve fibers to tones in noise near masked threshold. *Journal of the Acoustical Society of America, 79,* 426–442.
Zwicker, E., & Schorn, K. (1978). Psychoacoustical tuning curves in audiology. *Audiology, 17,* 120–140.

2

Representation of the Vowel /eh/ in the Auditory Nerve of Cats With a Noise-Induced Hearing Loss

Roger L. Miller
John R. Schilling
Eric D. Young
Department of Biomedical Engineering
The Johns Hopkins School of Medicine

Kevin R. Franck
University of Washington
Department of Speech and Hearing Sciences

A population study of single auditory-nerve fibers was used to characterize the deficits induced by a 2-hour exposure to narrow-band noise centered at 2 kHz (50 Hz bandwidth, 115 dB SPL). A period of 45 days was allowed for recovery from temporary threshold shifts. Single-fiber responses to the vowel /eh/ were recorded at intensities ranging from near the threshold of fibers in the damaged region (40–80 dB threshold shift) to a maximum of about 110 dB SPL. Tuning curves taken from fibers with best frequencies in the region of acoustic trauma showed a loss of sensitivity and a decreased Q_{10}, in agreement with previous studies. In normal animals, the temporal response pattern of fibers shows a capture phenomenon, in which the first two formant frequencies increasingly dominate the responses of fibers as stimulus level increases. By contrast, in exposed animals fibers respond to a broad range of frequencies and do not show capture by the formants. This result is consistent with broadened tuning, but probably also reflects a weakening of cochlear suppression.

INTRODUCTION

Previous studies of auditory nerve pathophysiology following noise or ototoxic damage to the cochlea demonstrated a loss of sensitivity at best frequency (BF) and a broadening of tuning curves (Kiang, Liberman, & Levine, 1976; Liberman & Mulroy, 1982; Robertson, 1982; Robertson & Johnstone, 1979). These changes have been related to specific damage to hair cells, especially to hair cell cilia (Liberman & Dodds, 1984b). Modifications of two-tone suppression have also been observed (Schmiedt, Mills, & Adams, 1990). The implications of these changes for responses to complex sounds such as speech have received little attention, although some studies have been done (Geisler, 1989; Palmer & Moorjani, 1993). The effects of loss of sensitivity are straightforward, in that responses to weak stimuli are not observed, but the implications of broadened tuning and loss of two-tone suppression are more difficult to predict. Studies of the temporal responses of auditory nerve fibers to vowel-like stimuli (Delgutte & Kiang, 1984; Palmer, 1990; Palmer, Winter, & Darwin, 1986; Sinex & Geisler, 1983; Young & Sachs, 1979) demonstrated a tendency for formant frequencies to capture the responses of auditory nerve fibers over a wide range of BFs. This capture phenomenon is nonlinear in that it is not predictable from the tuning properties of the fibers alone, and probably involves cochlear suppression phenomena to a considerable degree. In this chapter, we report on a population study of responses to the vowel /eh/ of auditory nerve fibers in cats with noise-induced cochlear damage. These fibers show dramatic differences from fibers in normal cats in terms of their temporal responses to the vowel. In particular, the capture effect is much weaker and the responses of fibers are more broadband than in normal cats.

METHODS

Healthy adult male cats, about 8 pounds in weight, with clean middle ears and translucent tympanic membranes were used. In preparation for noise exposure, animals were anesthetized by an injection (im) of 25 mg of acepromazine maleate mixed with 250 mg of ketamine. Additional doses were administered as needed. A noise band, centered at 2 kHz with 50 Hz bandwidth, was then presented for 2 hours at a level of 115 dB SPL in free field. Exposure was done with the animal positioned directly below two loudspeakers. The pinna transfer function, which is flat for a 2 kHz source in this position, produces an exposure of about 125 dB SPL at the tympanic membrane (Rice, May, Spirov, & Young, 1992). Following exposure, the animal was allowed to recover for at least 45 days to

eliminate temporary threshold shift. This period was judged to be sufficient based on a previous behavioral study of the effects of broadband noise exposure (Miller, Watson, & Covell, 1963).

In preparation for recording from the auditory nerve, animals were anesthetized by injection of xylazine (0.2 mg im) followed by ketamine (200 mg im). An areflexic state of anesthesia was maintained for the duration of the experiment by intravenous injections of pentobarbital. Physiological saline (≈1 ml/hr) and lactated Ringer's (≈10 ml/24 hrs) were given to prevent dehydration. Atropine (0.1 mg im) was given every 24 hours to control mucus secretions. A tracheotomy was performed to maintain an open, low-resistance airway, and to minimize respiratory acoustic artifacts. The bulla was vented with a 40 cm length of polyethylene tubing (PE-90) to prevent the buildup of negative pressure in the middle ear (Guinan & Peake, 1967). Rectal temperature was maintained at 38.5°C with a feedback-controlled heating pad.

Sound stimuli were delivered via an acoustic system similar to that designed by Sokolich (1977). In our system, the electrostatic driver was replaced with a 5-inch dynamic speaker, which increased the maximum tone presentation level to about 125 dB SPL. The frequency response for this system is relatively flat (± 6 dB) up to 10 kHz, which is sufficient for the study of auditory nerve fibers with BFs within the spectral range of the vowel.

Recordings were made in an electrically shielded, double-walled, soundproof room (IAC-1204A). Micropipettes of 10–30 MΩ were filled with 3M KCl and placed in the auditory nerve under visual control after retraction of the cerebellum medially. Single fibers were isolated by driving the electrode in 1–2 mm steps while presenting a broadband noise search stimulus (≈35 dB re 20 $\mu Pa/\sqrt{Hz}$).

For each fiber, the following data were taken: the frequency threshold curve (FTC), a sample of spontaneous activity, responses to a BF tone 50 dB above threshold, a measure of two-tone suppression, and responses to the speech stimulus. The speech stimulus used was the CVC syllable /besh/; only responses to the vowel portion /eh/ are reported here. This stimulus was presented 60–100 times at 1/s. Approximately 800 spikes were recorded in response to the vowel. The stimulus was presented at three sound levels, 20 dB apart, with a maximum vowel level of ≈110 dB SPL. We continued to record from fibers in an animal until a loss of sensitivity, relative to previous fibers of similar BF, was noticed.

The /besh/ was synthesized using a Klatt synthesizer (Klatt, 1980), implemented in the ACSL programming language (Franck, 1994). Formant frequencies were as follows: F1(0.5 kHz), F2(1.7 kHz), F3(2.5 kHz), F4(3.3 kHz), and F5(3.7 kHz), and were chosen to be at harmonics of the 100 Hz fundamental frequency of the vowel.

RESULTS

Thresholds and Tuning

Here we describe results from one population experiment, 95-01-27, in which 167 fibers were studied. Figure 2.1 illustrates the effects of the acoustic trauma on thresholds (Fig. 2.1A) and tuning bandwidth, as measured by Q_{10} (Fig. 2.1B), plotted against BF. There is some uncertainty in assignment of BF to fibers following acoustic trauma. We selected the frequency closest to the start of the high-frequency slope portion of the FTC, as opposed to the nominal BF, because this choice gives the best agreement with the basilar membrane frequency map following acoustic trauma (Liberman, 1984). In Fig. 2.1A, single fiber sensitivity is compared to the line marked LBTC, which represents the best threshold curve obtained by Liberman (1978) for cats unlikely to have been exposed to acoustic injury. Threshold shift was greatest for fibers in the 1.5 to 6 kHz range, although a reduced sensitivity of at least 15 dB was present for all sampled fibers.

The effects of our deafening paradigm were quite variable across cats. In some cats there was virtually no threshold shift, whereas in others threshold shifts of 80 dB or more were noted near 2 kHz. A large threshold shift at very low frequencies is not expected from this noise exposure (Liberman & Kiang, 1978). We consistently observed such shifts in cats obtained from the same supplier, so the sensitivity loss in this region may reflect a preexisting condition.

Figure 2.1B shows the Q_{10} of FTCs from the same cat, compared to published normal values: The solid lines show the range of Q_{10} measurements from Liberman (1984) and the dotted lines are from Evans and Wilson (1973). Notice the depressed Q_{10} values for BFs from 1.5 to 4 kHz. High Q_{10} values are seen in fibers with BF < 7 kHz, indicating sharp tuning. In fact, these fibers have Q_{10}s somewhat above the normal data.

In the following sections we describe abnormalities in the temporal response pattern for fibers grouped by their proximity to the major spectral features of a steady state vowel. Isolation was maintained long enough to allow characterization of the speech stimulus at three or two presentation levels for 40 or 65 fibers, respectively.

Synchrony to Multiple Harmonics Near F2

Figure 2.2 shows data from three fibers with BFs near F2; one fiber is from a normal cat and two are from an exposed cat. The fibers' FTCs are shown at the top left. These fibers were chosen for their proximity to F2; their BFs are slightly above or below 1.7 kHz, but the following results

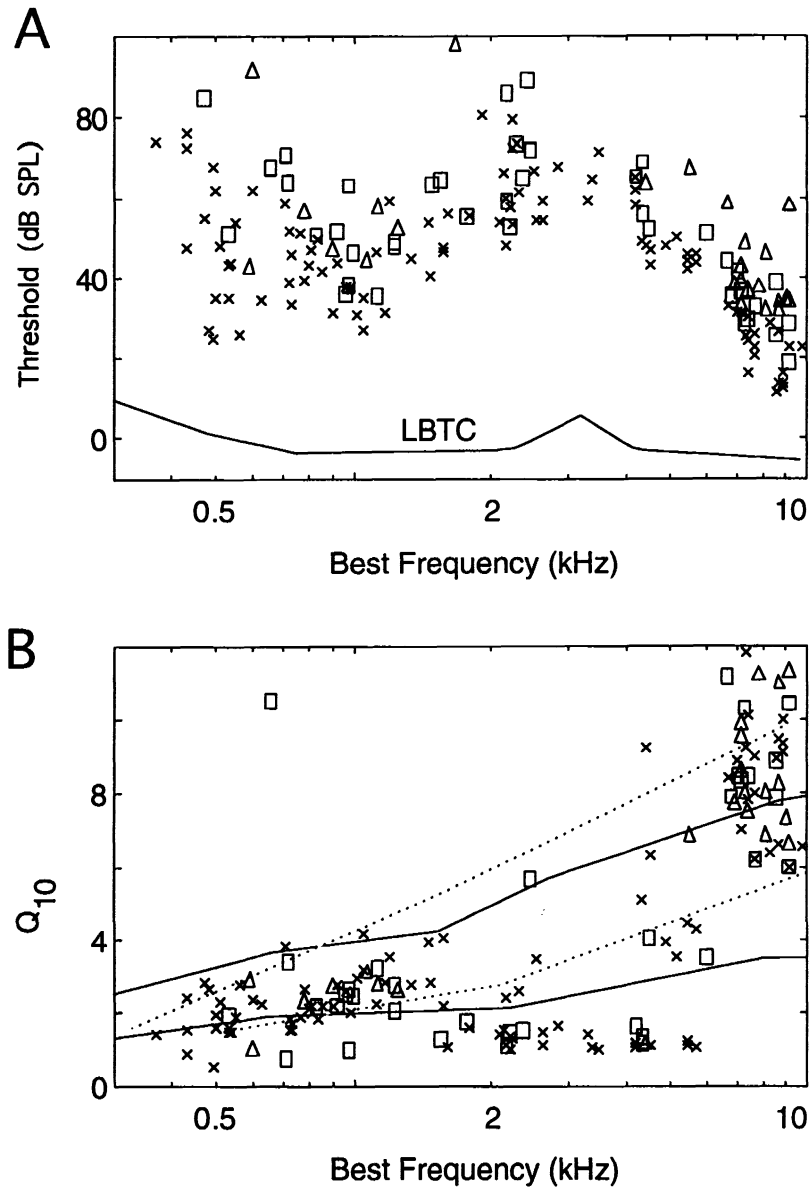

FIG. 2.1. FTC measures of acoustic threshold and tuning for the sample population of fibers from 95-01-27 compared to the expected limits for normal fibers shown by the lines, as explained in the text. A. Thresholds at BF show a shift of at least 50 dB for fibers near the noise-band center frequency (2 kHz) as compared to expected sensitivity, shown as a solid line (LBTC, from Liberman, 1978). B. Q_{10} measure of FTC width, defined as BF divided by FTC bandwidth 10 dB above threshold. The abundance of fibers with Q_{10} values below the normal range demonstrates a broadening of FTCs for fibers near the region of acoustic damage. Spontaneous rate (SR) firing rate classes are: X, high-SR, greater than 18 /sec; □, medium-SR, 1-18 /sec; Δ, low-SR, less than 1 /sec.